Energy Conversion and Management 298 (2023) 117684

Contents lists available at ScienceDirect

Energy Conversion and Management

journal homepage: www.elsevier.com/locate/enconman

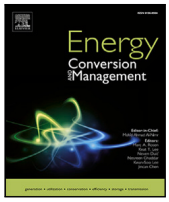

Modeling and simulation of nuclear hybrid energy systems architectures

Guido Carlo Masotti, Antonio Cammi, Stefano Lorenzi *, Marco Enrico Ricotti

Department of Energy, Politecnico di Milano, via La Masa, 34, Milano, 20156, Italy

ARTICLE INFO

Keywords:
Nuclear hybrid energy system
Small Modular Reactor
Cogeneration
Flexible operation
Modelica

ABSTRACT

The transition toward a low-carbon energy system and the increasing penetration of variable renewable energy (VRE) sources translate into a pressing need for dispatchable and low-carbon power sources. Nuclear hybrid energy systems (NHES) exploit the synergies between nuclear power and other energy sources together with energy storage devices and a variety of electric and non-electric applications. The expected benefits range from a high flexibility being able to supporting an increasing penetration of the VRE while complying with the grid demand and constraints to an increased profitability brought by the production of commodities beyond electricity (e.g., hydrogen, heat, etc.).

A dedicated framework must be developed to evaluate different NHES configurations, particularly with regard to the complex interconnections among the tightly coupled components. In this work, illustrative examples of NHES components were selected and modeled with the object-oriented modeling language Modelica and implemented in the Dymola simulation environment. The technologies considered in this study are a Small Modular Reactor (SMR) based on pressurized water technology, a thermal energy storage (TES) system, and an alkaline electrolyzer for hydrogen production. The dynamic models are then collected in a new Modelica library and assembled into a variety of NHES topologies using a plug-and-play approach. The time-dependent behavior of the NHES layout can be simulated under different operational contexts, enabling the monitoring of key process variables, supporting system design, exploring alternative control strategies, and analyzing different scenarios.

The NHESs are investigated in two exemplary scenarios – one representing typical load conditions and the other featuring high VRE penetration – in order to demonstrate the viability of the proposed approach as an initial effort toward the development of a holistic framework for analyzing NHES. The dynamic models effectively met the analysis requirements, for instance, by tracking the production of commodities throughout each operational transient, which is an essential result for evaluating the performance of NHES. In this regard, efficiency is adopted as the figure of merit to compare the different NHES architectures, with simulation results indicating significant overall efficiency improvements in NHES incorporating TES and using nuclear heat to drive non-electric applications.

1. Introduction

Energy demand is expected to grow in the future, driven mainly by the increasing global population and economic activity [1]. This surge must be tackled while addressing the so-called energy trilemma, which entails energy security, affordability, and sustainability. In the context of climate change, sustainability is closely tied to a reduction of greenhouse gas (GHG) emissions, which can be achieved by deploying low-carbon energy sources, such as nuclear energy and renewable energy sources, both to meet rising energy demand and phase out fossil-fueled generators.

According to the projections presented by the Intergovernmental Panel on Climate Change (IPCC) [2] and the International Energy Agency (IEA) [3], a substantial rise in renewable energy and nuclear capacity is foreseen in order to meet climate goals. Among renewable energy systems, wind and solar power are predicted to expand rapidly, mainly thanks to their low marginal production costs, low GHG emissions during their lifecycles, and increased scalability potential with respect to other renewable energy sources, such as hydroelectric power, which is limited by the available natural resources [3]. However, there are several concerns to address in the case of a considerable penetration of variable renewable energy sources (VRE) in the energy mix, most of which are connected to their intermittent nature [4]. Their power production is non-programmable since it is dependent on meteorological conditions, which can vary in both time and location and may result in a mismatch between power supply and load demand. The fluctuations and uncertainties in the VRE's power output represent a major

* Corresponding author.
E-mail address: stefano.lorenzi@polimi.it (S. Lorenzi).

https://doi.org/10.1016/j.enconman.2023.117684
Received 24 May 2023; Received in revised form 3 September 2023; Accepted 18 September 2023
Available online 24 October 2023

Nomenclature

$\dot{m}$	mass flow rate (kg s^{-1})
$\dot{Q}$	thermal power (W)
A	area (m^2)
c_i	density of the ith precursor group (m^{-3})
c_p	specific heat capacity (J kg^{-1} K^{-1})
d	density (kg m^{-3})
E	energy (J)
H	enthalpy (J)
h	specific enthalpy (J kg^{-1})
k	thermal conductivity (W m^{-1} K^{-1})
K_v	hydraulic conductance (kg s^{-1} Pa^{-1})
L	length (m)
M	mass (kg)
n	neutron density (m^{-3})
P	power (W)
p	pressure (Pa)
q'''	power density (W m^{-3})
r	radius (m)
T	temperature (K)
t	time (s)
V	volume (m^3)
v	voltage (V)
x	steam quality (-)

Acronyms

AEC	alkaline electrolyzer cell
BOP	balance of plant
EU	European Union
GHG	greenhouse gas
HP	high pressure
IHX	intermediate heat exchanger
LP	low pressure
LWR	light water reactor
MSR	moisture separator reheater
NHES	nuclear hybrid energy system
OTSG	once through steam generator
PCHE	printed circuit heat exchanger
PEM	proton exchange membrane
PHE	plate heat exchanger
PV	photovoltaic
PWR	pressurized water reactor
SMR	Small Modular Reactor
SOEC	solide oxide electrolyzer cell
TES	thermal energy storage
VRE	variable renewable energy source

Greek symbols

β	delayed neutron precursors fraction (pcm)
η	efficiency (-)
Λ	neutron generation time (s)
λ_i	decay constant of the ith precursor group (s^{-1})
ρ	reactivity (pcm)
τ	time constant (s)
θ	valve opening (-)

Subscripts and superscripts

a	anode
c	cathode
cl	cladding
f	fuel
$fric$	friction
g	gap
iso	isentropic
l	liquid
mec	mechanical
$stat$	static head
v	vapor
vl	vapor–liquid exchange
w	wall
sat	saturation
act	activation
bub	bubble
FL	flashing
ohm	ohmic
rev	reversible
RO	rain out
SC	superficial condensate
SP	sprayers
SRG	surge line
VLV	relief valve
WC	wall condensate

challenge for the integration of these sources in the electrical grid, since the mismatch between power supply and demand leads to grid instabilities, which in turn translate into higher system costs and the need for backup energy sources and energy storage systems [5]. Nuclear power, as a dispatchable and low-carbon energy source, may boost a deeper penetration of VREs in the energy mix by coping with their intermittency while also contributing to the decarbonization of the energy system. Traditionally, nuclear power plants have been operated in baseload mode, with their power output remaining at a nominal level regardless of load demand. In this case, load following is performed by modulating the power output of other programmable generators. Nonetheless, experiences in France and Germany, for example, demonstrated that nuclear reactors could provide some grid stability by varying the plant's power supply based on grid requirements [6].

The increasing penetration of VREs in the energy mix inevitably translates into higher flexibility requirements for programmable generators [5]. In the case of nuclear power plants, flexibility may be increased by deploying Small Modular Reactors (SMR), whose multi-modularity allows for an additional degree of freedom in power generation [7]. These reactors, similarly to conventional nuclear power plants, can be integrated into so-called nuclear hybrid energy systems (NHES), which provide a higher level of flexibility by assigning the produced energy to applications other than electricity supply in accordance with grid requirements.

1.1. Nuclear hybrid energy systems

In a NHES, the flexibility is increased by combining the nuclear reactor with other energy sources, energy storage systems, and applications beyond electricity supply, including hydrogen production, district heating, desalination, and process heat supply [8]. As a result, in addition to delivering dispatchable power to the grid, the system gains access to multiple markets, allowing it to be managed to supply the most profitable energy product at any given time in order to maximize the revenue streams [9].

Table 1
Operating temperatures of Generation IV reactor concepts [10].

Reactor concept		Temperature range (°C)
Lead-cooled fast reactor	LFR	480–570
Sodium-cooled fast reactor	SFR	500–550
Supercritical water reactor	SCWR	510–625
Molten salt reactor	MSR	700–800
Gas-cooled fast reactor	GFR	850
Very high temperature reactor	VHTR	900–1000

Generally speaking, cogeneration can have a significant impact on the economic competitiveness and flexible operation of nuclear power plants. For instance, it enables the direct exploitation of the reactor's thermal energy, which, in a conventional steam cycle, would be converted into electricity and discharged into a cold sink. As of today, there have been several experiences with nuclear power plants employed for cogeneration purposes, mainly desalination, district heating, and process heat supply [10]. Other viable cogeneration alternatives include hydrogen production and coupling with chemical processes, as well as hard-to-abate industrial sectors such as steel, glass, ceramics, and pulp and paper manufacturing. The latter industrial processes require high-quality heat in a temperature range of 600–1200 °C [10]. These temperatures are hardly achievable with LWR technologies, where the steam outlet temperature is usually below 300 °C. However, as pointed out in Table 1, these temperature requirements can be met by using Generation IV reactors, which employ unconventional coolants such as molten salts, liquid metals, or gas [7].

When integrated with cogeneration processes, the reactor can be operated in load following by cogeneration mode [10]. In this operational setting, the thermal power output of the reactor is maintained at its rated power, while the electric output is modulated by diverting the excess power for cogeneration purposes. As a result, it is possible to satisfy a variable load profile while also benefiting from the technological and economic advantages of running the reactor at nominal conditions.

Fig. 1 shows a possible NHES architecture. This particular configuration is known as "tightly coupled", since the nuclear reactor, the renewable energy sources, the energy storage systems, and the industrial processes are coupled upstream of the interconnection point with the electrical grid. Other layouts are based on the "thermally coupled" approach, in which only the nuclear reactor is thermally interconnected with industrial facilities, or the "loosely coupled" philosophy. Current energy systems are based on the latter approach, since the generators are managed independently from each other to meet certain grid requirements [11].

The design of a NHES, in terms of both technologies and the capacities of interconnected subsystems, is strongly dependent on the operational context. The boundary conditions, i.e., load demand, environmental conditions, as well as energy product market dynamics and energy policies in the given location, are essential to determining the suitability of the considered NHES layout. This is not only true for system design but also to establish the best operation conditions for NHES since it will affect the energy dispatch strategy that maximizes the system's profitability.

Among the potential technologies to be integrated into a NHES, SMRs are looked at with remarkable interest [13]. SMRs are defined as reactors with a lower power capacity with respect to conventional reactors, usually below 300 MWe. This feature allows for a higher degree of modularity and scalability, so that multiple SMR modules can be installed in the NHES and be operated independently to meet different grid requirements [7]. The reactors rely on an integral design, meaning that the primary loop is packed in the pressure vessel. This greatly improves the safety of the system, mainly because of the reduced number of vessel penetrations and the adoption of passive safety

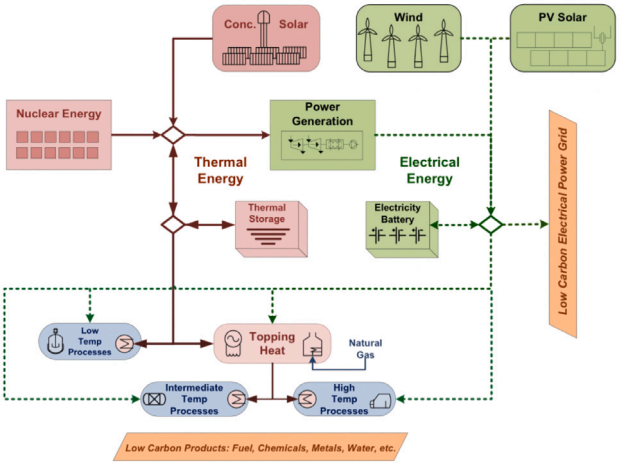

Fig. 1. Tightly coupled NHES structure [12].

systems such as natural circulation of the primary coolant. Moreover, because of their smaller size and high safety degree, SMRs require a reduced emergency planning zone. The importance of the latter aspect is particularly significant when integrating SMRs in NHES, as it enables the SMRs to be located closer to industrial sites.

Several studies are available in the literature concerning the analysis of NHES. For instance, Garcia et al. [14,15] compared two NHES architectures, one labeled "traditional" including a heat source, a wind farm, and battery storage, and the other incorporating also a chemical plant driven by thermal power extracted from the aforementioned heat source. This study primarily aimed at investigating the potential of flexible operation in these systems to cope with varying levels of VRE penetration, both from a technical [14] and economic standpoint [15]. Kim et al. [16] showcased an example of coupling an SMR with a hydrogen production process within a NHES. The study demonstrated the technical feasibility of meeting fluctuating load demands by allocating thermal and electrical power flows for hydrogen production. Another end-user process that could be integrated into NHES is desalination. This option is explored in the analysis conducted by Hills et al. [17], where NHES connecting a SMR and a wind farm with either freeze desalination or reverse osmosis are compared. The opportunities of integrating the Palo Verde nuclear power plant in Arizona into a NHES were investigated by Epiney et al. [18]. Through the analysis of various case studies with different levels of desalination plant utilization, the viability of investments to cope with the intermittency of renewables and ensure the supply of cooling water for the nuclear power plant is evaluated. NHES modeling presents several significant challenges, as highlighted by the extensive research conducted in this field. Such challenges are primarily driven by the complex interconnections between multiple subsystems and the highly dynamic nature of their operations. Moreover, the complexity increases when performing a techno-economic optimization of the energy system, as it requires taking into account interactions with several energy output markets [19].

As of today, NHES are under investigation in various research initiatives. The Task Force on Non-Electric Applications of Nuclear Heat (NEANH), established within the Generation IV International Forum (GIF), is dedicated to exploring the potential of Generation IV reactors in supplying heat for applications beyond electricity supply [20]. In particular, the significance of having tightly coupled NHES to enhance the flexibility of the overall system and to provide high-quality heat as a valuable commodity is emphasized [20]. Euratom's TANDEM (Small Modular ReacTor for a European sAfe aNd Decarbonized

Energy Mix) is spearheading the exploration of NHES in the European Union, coordinating the research activities of EU Member States with particular attention to the safety concerns of integrating light-water cooled SMRs into NHES [21]. Moreover, activities related to modeling and simulation for the techno-economic evaluation and optimization of NHES are carried out by the Integrated Energy System program, run by the U.S. Department of Energy (DOE) [9]. In the latter programs, the development of dynamic models is a backbone for the analysis of NHES. Dynamic models are needed to simulate the system's behavior over time in response to different scenarios. They are required to assess if the subsystems, interacting with one another, are able to satisfy the commodity demands and the technical requirements. As a result, the models can be employed to identify potential issues in terms of system design and operation, as well as to estimate the NHES performance in various operational contexts. Lastly, dynamic models are a fundamental tool for the development of control strategies since they allow for the simulation of an energy dispatch in compliance with the technical constraints of the subsystems and for the optimization of the systems' performances [17].

The aim of this paper is to present some models of the components involved in NHES and their potential use in the analysis and simulation of different architectures. The dynamic models of NHES subsystems are developed in the object-oriented modeling language Modelica [22]. They are collected in a dedicated library, which will be successively used to assemble the models of different NHES architectures in line with a plug-and-play philosophy. With respect to previous studies on NHES, the primary focus of this work lies in highlighting the benefits of utilizing the latter approach. The key advantage stems from the smooth integration of individual subsystem models into comprehensive NHES models, enabling the exploration of a wide range of case studies.

The paper is organized as follows. In the next section, a possible methodology for the analysis of NHES is presented, focusing on the role of dynamic models in this framework. As illustrative examples of subsystems that can be integrated into a NHES, a SMR, a thermal energy storage system, and a hydrogen production unit were selected. These technologies are described and compared with other options in Section 3, while the implementation of their dynamic model is presented in Section 4. The resulting models are assembled into five different NHES architectures, which are illustrated in Section 5. Following the presentation of the scenarios that will be used to evaluate the dynamic behavior of the systems in Section 6, Section 7 summarizes the simulation results for the two most comprehensive configurations. Lastly, conclusive remarks about the outcomes of this work are discussed.

2. Methodology

The models presented in this work are meant to be used as tools in a broader framework for the analysis of NHES. For instance, the feasibility of incorporating SMRs in NHES can be assessed using a exhaustive techno-economic analysis that includes a safety assessment to determine if the SMR's safe operation is not jeopardized when it is interconnected with other components of the NHES [23].

A broad framework allows for the identification of the most appropriate NHES architecture as well as its operation, e.g., in terms of energy dispatch among the various NHES components in several scenarios. It can represent a valuable tool also for policymakers to evaluate the performance of NHES and estimate their potential for the transition towards a clean, reliable, and safe energy system.

2.1. Dynamic modeling of NHES components

As previously stated, the focus of this paper is on the development of dynamic models of NHES components, which will then be combined to assemble the dynamic model of overall NHES architectures. They were built in Modelica, an object-oriented modeling language that enables the development of easily interchangeable models and libraries [22]. The Modelica language can be coded in various simulation environments. The models proposed in this work were developed in Dymola® (Dynamic Modeling Laboratory), which relies on a proprietary license. Compatibility with the open-source environment OpenModelica is possible for the models, but it is important to note that the computational performances may differ given the use of different solvers in the two tools.

Thanks to its object-oriented language features, Modelica is particularly well suited for the simulation of large and complex engineering systems such as NHES. In particular, the encapsulation and abstraction principles allow for the independent implementation of submodels, which can then be linked through dedicated interfaces, also called connectors [22]. In this way, it is possible to easily reuse the same model with different parameters and boundary conditions. Furthermore, as an acausal language, Modelica provides high modeling flexibility and efficiency since inputs and outputs are not defined a priori.

Along with the Modelica Standard Library, two additional libraries, both designed at Politecnico di Milano, were applied to develop the models in this work. The NuKomp library [24], in particular, provides components for nuclear power plant modeling, whereas the ThermoPower library [25] is used for dynamic modeling of thermal power plants and energy conversion systems.

It is worth noting that the main objective of the Modelica model of the reactor is to forecast its dynamics in various contexts and to monitor the operational variables, while it is not meant for safety assessments.

2.2. Scenario development and implementation

The generation of reasonable scenarios is fundamental for assessing the technical and economic viability of integrating SMRs with multiple end-user applications and the overall NHES performances. A scenario encloses different boundary conditions that will affect the NHES design and operation, such as load demand, weather conditions, renewable energy source penetration, other generators in the energy mix, cogeneration product demand, and market dynamics. Of course, this operational context will be strongly dependent on the NHES location.

The primary goal of testing the NHES model against various scenarios is to determine whether the system's operation complies with technical constraints, such as ramping-up requirements to follow changes in load demand. In this work, the NHES models were tested with two load profiles, one representative of the current load profile and another characterized by a high penetration of solar power. These are intended just to investigate the response of NHES architectures to plausible load demand fluctuations and are not supposed to be representative of a real operational context, which entails a detailed examination of the local energy mix and its future forecasts, for instance.

2.3. Evaluation of system response

After assembling the models described in this work into multiple NHES architectures, they were tested in relation to the aforementioned scenarios. The simulation outcomes enable monitoring whether the system's process variables remain within their operational limits and provide quantitative information to evaluate system performances, such as assessing the amount of energy dispatched to each subsystem during operation.

The work presented in this paper is a preliminary contribution to the broader framework of NHES analysis since it focuses just on the methodology adopted for the dynamic modeling part. A thorough development of the scenarios, as well as the coupling with optimization tools and thermal-hydraulic system codes for the safety assessment of the system, goes beyond the scope of this work.

Table 2
Main parameters of a SMR module [28].

Parameter	Value	Unit
Thermal power	540	MWth
Electrical power	170	MWe
Pressure (primary/secondary)	150/45	bar
Core inlet/outlet temperature	280/307	°C
Primary mass flow rate	3700	kg/s

3. Technologies

The technologies to be integrated in the NHES architectures considered in this study include a light-water cooled SMR, a thermal energy storage system, and a hydrogen production plant.

These are just a few examples of potential technologies that can be considered for NHES. In particular, they can be seen as representative technologies for the nuclear energy source, an energy storage device, and the production of an additional commodity beyond electricity, respectively.

3.1. Small modular reactors

The reference configuration of the SMR considered in this work relies on a pressurized, light-water-cooled SMR (LW-SMR) design under investigation in Euratom's ELSMOR (Towards European Licensing of Small Modular Reactors) project, where a database with the key parameters for the European SMR (E-SMR) has been conceived [26]. The LW-SMR proposed in the framework of this project is guided by the principles of the NUWARD™ design, which is currently being developed by a consortium formed by CEA, EDF, Naval Group, TechnicAtome, Framatome, and Tractebel/Engie [27].

The main parameters considered for a single SMR module are summarized in Table 2. The nuclear power plant is planned to have a twin-module configuration that will enable it to house two 170 MWe units, each equipped with its own turbogenerator, in the same location [28]. However, in this study, only one module is considered as the primary energy source.

The high degree of compactness of the SMR is achieved by packing the entire primary circuit components within the integrated pressure vessel. Employing compact steam generators, such as Plate Heat Exchangers (PHE) or Printed Circuit Heat Exchangers (PCHE), enables the transfer of large amounts of thermal power in a small volume [29]. Six of these steam generators will be employed during normal operation in the LW-SMR, while two additional safety steam generators will cool the reactor in accidental conditions [28].

The considered layout employs six primary coolant pumps at the outlet of each steam generator to force the circulation of the coolant. On the other hand, the decay heat removal system is based on natural circulation, which translates into a higher degree of safety for the overall system due to this passive safety mechanism.

3.2. Energy storage

Energy storage systems hold a decisive role in balancing grid supply and demand and reducing curtailed energy. There are several methods to store energy, e.g., mechanically, electrically, electrochemically, chemically, or thermally. Among these, the storage of mechanical energy with pumped storage hydropower is the most widespread alternative [30].

In this study, a thermal energy storage system was selected to be coupled with the SMR in the NHES. This technology is particularly well-suited to being integrated with nuclear power plants since it allows storing the thermal energy produced by the reactor without undergoing intermediate transformations. Thermal energy storage systems can rely on different physical processes [31]:

- Sensible heat storage: the liquid or solid storage medium is heated by the energy sources without undergoing phase change. As a result, changes in temperature arise from energy absorption and release.
- Latent heat storage: in this system, heat drives the phase transition of the sensible medium, which occurs at isothermal conditions.
- Thermochemical storage: the exchanged heat activates endothermic and exothermic chemical processes, storing energy as chemical potential.

As of today, experience with large-scale thermal storage units is available when coupled with concentrating solar-thermal power (CSP). In this context, sensible heat storage systems based on the two-tank configuration and employing molten salts as a storage medium are considered the most mature technology. This same option is regarded as the most promising when coupled with a SMR as well [32].

Storage media are typically selected based on favorable material properties, such as high thermal conductivity, density, and heat capacity, low melting point, mechanical and chemical stability, and low costs [31]. The most common molten salt used for this application, also known as solar salt, is in compliance with all these requirements. However, it is not compatible with LW-SMR since its minimum operation temperature, around 290 °C [33], is not compatible with the steam line temperature of the reactor, resulting in a too small temperature margin. As a result, the synthetic oil Therminol-66 is considered for this type of application, despite its higher costs and increased safety concerns [32].

3.3. Hydrogen production

Hydrogen demand is expected to grow significantly in the future, mainly thanks to its versatility and potential use for the decarbonization of hard-to-abate sectors. This energy carrier can be produced to store energy, which can then be recovered using hydrogen itself as fuel. Moreover, it can be employed as fuel in the transportation sector or as chemical feedstock for industrial processes [34].

The contribution of hydrogen to the energy transition is closely linked to its production method. As of today, the most widespread process is steam methane reforming, in which the reaction of steam and methane produces hydrogen with the emission of CO_2 as a by-product. Water splitting by electrolysis is suggested for producing low-carbon hydrogen since the hydrogen generation process requires just electric power as input.

Among the technologies based on this technique, the alkaline electrolyzer cell (AEC) is the most mature alternative. It is characterized by a low operating temperature, usually in the range of 60-90 °C [35]. An electrolyzer stack contains an anode and a cathode, which are the positive and negative electrodes, respectively. At the cathode, water is divided into hydroxide anions and hydrogen. The anions are attracted by the cathode, where they are oxidized into water and oxygen [36]:

$$2H_2O(l) + 2e^- \rightarrow H_2(g) + 2OH^-(aq) \quad \text{(Cathode)}$$

$$2OH^-(aq) \rightarrow \frac{1}{2}O_2(g) + H_2O(l) + 2e^- \quad \text{(Anode)}$$

The main feature of an alkaline electrolyzer is that the electrolyte, the medium through which the ions move, is liquid. In particular, it is an aqueous solution of potassium hydroxide at a weight concentration of 20%–30%, which increases the material's electrical conductivity while minimizing its corrosive impact on the other components.

Hydrogen production systems based on AECs have the disadvantage of having a low flexibility, so that they are mainly used for steady state operation. Nonetheless, it is worth highlighting that the development of alternative electrolysis technologies, including proton exchange membranes (PEM) and solid oxide electrolysis cells (SOECs), is rapidly

advancing. The former exhibits high load ramping capabilities, enabling it to effectively manage fluctuating power inputs [37]. On the other hand, SOECs operate at temperatures above 600 °C, resulting in a more efficient hydrogen production process.

4. Modeling of the NHES components

This section describes the modeling of the aforementioned technologies in Modelica. The encapsulation property of this modeling language is extensively employed for each model, resulting in the independent modeling of the key elements of each technology and their subsequent assembly into the overall model.

In addition to the Modelica Standard Library, most of the components stem from the ThermoPower library, especially from the *Water* package, which includes models describing a one-dimensional fluid flow in a tube, discretized according to the finite volume (`Flow1DFV`) or finite element (`Flow1DFEM`) method, accumulation volumes (`Mixer`, `Header`, etc.), as well as valves and turbines, for example. This package relies on the fluid properties provided by the Modelica Standard library, which computes the properties for single- and two-phase water according to the thermodynamic state of the fluid.

4.1. LW-SMR

The model developed to simulate the behavior of the SMR is shown in Fig. 2. The main components, namely the core, the pressurizer, and the steam generator, were modeled independently and connected subsequently through dedicated interfaces. These components, together with the riser, the downcomer, and the upper and lower plena, rely on the models provided by the ThermoPower library. As far as the core is concerned, it was simulated using the model of the NuKomp library.

It is worth noting that the model is built upon the available E-SMR parameters, while others were assumed within the scope of this study as outlined in the following sections. Due to the absence of reference studies or experimental data that can be used to directly compare the simulation outcomes obtained with the proposed dynamic models, the E-SMR and its balance of plant models cannot be properly validated in this study. Nevertheless, the inherent uncertainties resulting from the simulations are accepted since the main objective of this work is to showcase the dynamic modeling of NHES architectures by means of a plug-and-play philosophy rather than providing an accurate description of the system's behavior.

4.1.1. Core

This component is composed of three submodels, representing (i) the neutronics, (ii) the fuel pin thermal behavior, and (iii) the coolant flow [24]. The main equations governing these submodels are available in Appendix A.

The neutronics of the system relies on point kinetics equations, together with reactivity feedback mechanisms. As a first approximation, only the Doppler and moderator feedback effects, which are related to the fuel and coolant temperatures, respectively, were taken into account. Moreover, an additional reactivity contribution, representing the insertion or extraction of control rods, can be specified through an external input.

To model the thermal behavior of the fuel pins, the fuel is divided into axial volumes, and in each volume, the one-dimensional, time-dependent heat equation is solved to find the radial temperature distribution. The heat equation is applied to five different radial zones: three are dedicated to the temperature distribution in the fuel pellet, while the other two describe the heat transfer in the gap and in the cladding.

Finally, a specific model is used to describe the coolant flow through the core channels. It is modeled by modifying ThermoPower's `Flow1DFV` component, in which energy, mass, and momentum balance equations are solved to determine the dynamics of the flow between the fuel pins, by including a connector representing the moderator feedback on the neutron kinetics. In addition, it is thermally linked to the fuel pin submodule in order to account for the thermal power transferred from the fuel pins to the coolant.

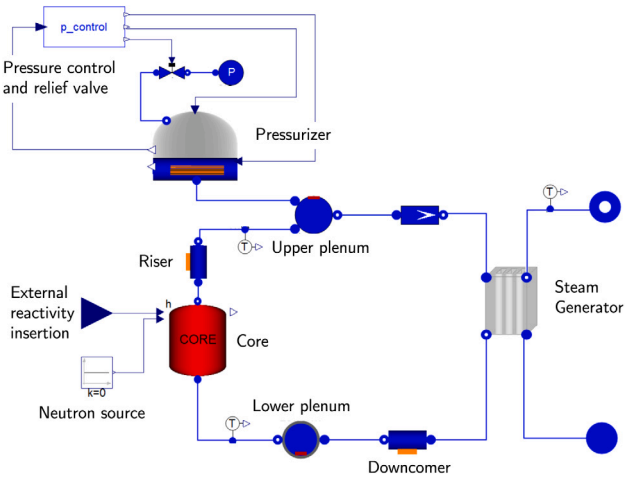

Fig. 2. Dynamic model of the SMR.

4.1.2. Pressurizer

In nuclear reactors employing PWR technology, the pressurizer is a key component to control the pressure in the primary loop and maintain the coolant in the liquid state. The model proposed in this work is based on the mathematical framework developed for the dynamic model of the IRIS (International Reactor Innovative and Secure) reactor [38]. IRIS is a PWR-type SMR, and, similarly to the LW-SMR considered in this work, its pressurizer is integrated within the pressure vessel. A non-equilibrium, two-region thermodynamic model was implemented to simulate the dynamics of the system. With this approach, the energy and mass balance equations are solved separately for the liquid and vapor regions as reported in Appendix A [39]. The same model can also be applied to a conventional PWR; however, the geometrical features must be corrected to account for the cylindrical shape [39] rather than the peculiar hemispherical shape in the SMR case.

In this work, the dynamic model of IRIS' pressurizer was adapted to account for the E-SMR's different geometry and pressure control scheme. As a matter of fact, the bottom part of the IRIS pressurizer consists of an annular chamber, which is required to house the pumps at the steam generator inlet. On the other hand, in the configuration proposed for the E-SMR, the primary coolant pumps are located at the steam generator outlet [28], meaning that the previous annular space is integrated within the pressurizer.

As far as the pressure control strategy is concerned, sprayers and an electrical heater were included in the model to lower and increase the pressure, respectively. Moreover, a pressure relief valve that is opened whenever the pressure crosses a certain threshold is considered. Similarly for the sprayers and the heater, logic signals are employed to activate and deactivate these control systems to keep the pressure in an acceptable range. In the control strategy, the sprayers feature a mass flow rate injection of 1.91 kg/s, while the thermal power provided by the heater is 80 kW [39]. During normal operation, these control systems are activated or deactivated based on the deviation of the primary coolant pressure from predetermined pressure setpoints. Sprayers were added to the IRIS pressurizer model because the design of this reactor, owing to its low core power and significantly larger steam header volume, allows the use of sprayers to be avoided [40].

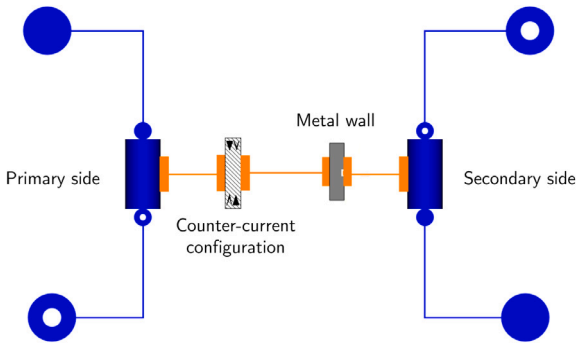

Fig. 3. Dynamic model of the steam generator.

4.1.3. Steam generator

The PCHE is the reference configuration selected for the steam generator employed in the considered LW-SMR. In the this design, the primary and secondary coolants flow through mini-channels with a rectangular or semi-circular cross section, which translates into enhanced heat transfer capability and thus compactness of the heat exchanger [29].

A preliminary sizing procedure is proposed to ensure that the steam generators fit within the available volume and meet the heat transfer requirements. In particular, the total cross-sectional area of each PCHE is determined to be consistent with the space available in the annular region of the integrated pressure vessel. On the other hand, the required steam generator length is tuned so that, at nominal operating conditions, the heat transfer capability of the heat exchangers allows for the transfer of the required thermal power. The steam generator geometry obtained employing the channel dimensions provided by literature [29], i.e., channels with a 4 mm wide and 2 mm high rectangular cross section, are summarized in Table 3.

The structure of the steam generator model in Modelica is reported in Fig. 3. It relies mainly on models that stem from the ThermoPower library, specifically the `Flow1DFV` component, which is used to simulate the primary and secondary coolant flow dynamics in the PCHE channels. These submodels are thermally linked with each other through a component representing the thermal behavior of the steam generator's solid structure, i.e., in terms of heat capacity and thermal resistance, and an additional component that accounts for the counter-current configuration of the considered PCHE design.

The ThermoPower `Flow1DFV` component allows the user to specify the heat transfer model employed on the hot and cold sides of the heat exchanger. In this work, the Dittus-Boelter correlation [41] was implemented to compute the heat transfer coefficient on the primary side, while a constant heat transfer coefficient determined with the Kandlikar correlation [42] was employed to model the secondary coolant evaporation.

4.1.4. Overall primary circuit model

Combining the models described in the previous sections, the overall model of the SMR shown in Fig. 2 is obtained. It is complemented with additional components of the ThermoPower library to simulate the primary coolant flow in the riser, downcomer, and upper and lower plena. The model is linked with other components through an external input that allows for the specification of the reactivity insertion through control rods and two flanges that represent the secondary coolant flow at the steam generator inlet and outlet. These flanges are the interfaces through which the model can be connected to the balance of plant, for instance.

The main simplifying assumption on which this primary circuit model is based is that the pressure drops experienced by the primary coolant flow through the components were neglected. This hypothesis simplifies the model by eliminating the need to include the primary pumps, which are required to counterbalance the pressure drop. The validity of this assumption finds support in the operational conditions examined in the proposed case studies, where the reactor operates in load following by cogeneration. During normal operation, this mode prevents the occurrence of severe transients that could significantly impact pressure drop distribution.

Table 3
Main parameters employed in the SMR model.

Parameter	Value	Unit
Steam Generator		
Number of channels	35552	/
PCHE cold side inlet/outlet temperature	247.44/287.44	°C
Length	2.61	m
Height	0.53	m
Width	1.015	m
Balance of plant		
Secondary mass flow rate	294.73	kg/s
Turbine stage inlet pressure (HP/LP)	45/11.05	bar

4.1.5. Reactivity insertion transient

The physical behavior of the proposed dynamic model is tested by simulating the system's response to a transient triggered by the injection of reactivity.

Fig. 4 shows the dynamic response of the SMR with respect to a step-wise 100 pcm reactivity insertion after 10 s. The proposed scenario involves connecting the steam generator inlet and outlet flanges, depicted on the right-hand side of Fig. 2, to an ideal flow source and sink, respectively. Before the transient is triggered, the system is in steady state and at values that are in agreement with the reference data provided for the reactor, reported in Table 2. The reactivity insertion results in a sudden increase in thermal power, causing the fuel and coolant temperatures to rise. This, in turn, triggers negative reactivity contributions through feedback mechanisms, as depicted in Fig. 4(b). In a short timescale, the Doppler feedback, followed by the moderator feedback, compensates for the external reactivity insertion, allowing the system to achieve a new steady state condition. However, it is worth noting that the modeling assumptions have a significant impact on this trend. The latter is affected not only by the primary circuit's underlying hypotheses but also by those of the cold side of the steam generator, such as the ideal flow source and sink, as well as the assumption of a constant heat transfer coefficient. They will have a significant impact on the steam generator's heat removal capability, thereby affecting the temperature increase and feedback reactivity contribution of the fuel and primary coolant.

4.2. Balance of plant

A steam cycle is employed to convert the thermal power produced by the SMR into mechanical energy. The reference balance of plant (BOP) considered in this study is the one proposed for the IRIS reactor [43]. It is based on a double-flow high-pressure (HP) and low-pressure stage (LP) turbine with different steam extraction points intended to power feedwater heaters and reheaters.

A simplified model of the BOP is implemented in Modelica. Only one steam extraction point, located before the HP turbine inlet, is present. The steam diverted at this point is used in a reheater positioned after a moisture separator between the two turbine stages. Indeed, only the two turbine stages and the moisture separator reheater (MSR) were included in the model. As a result, the power conversion system can be seen as an "open cycle": the secondary coolant flow is generated by a mass flow source connected to the steam generator inlet, while it is discharged in a sink at the turbine outlet. Therefore, the coolant flow in the other main components of the steam cycle, such as the condenser,

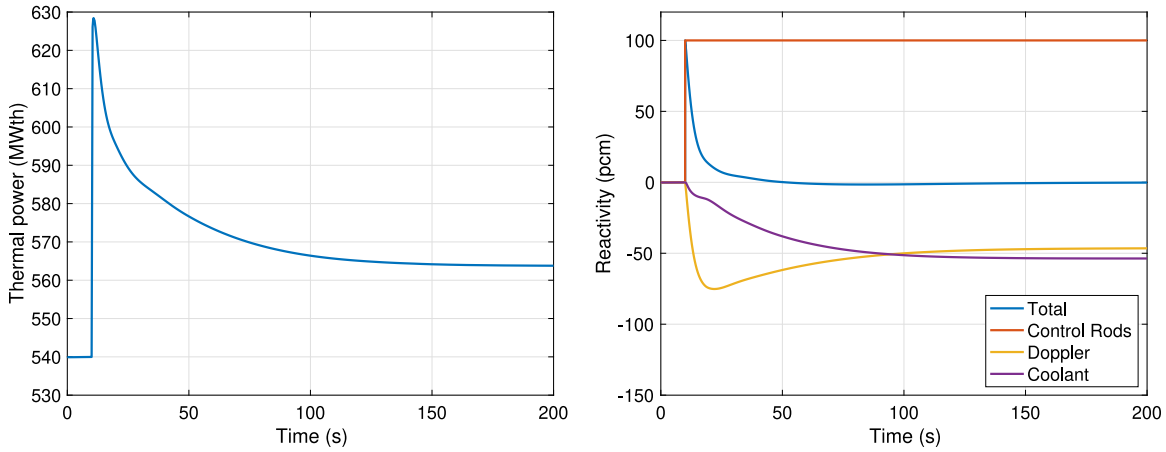

(a) Reactor power. (b) Reactivity contributions.

Fig. 4. Simulation results with a 100 pcm reactivity insertion.

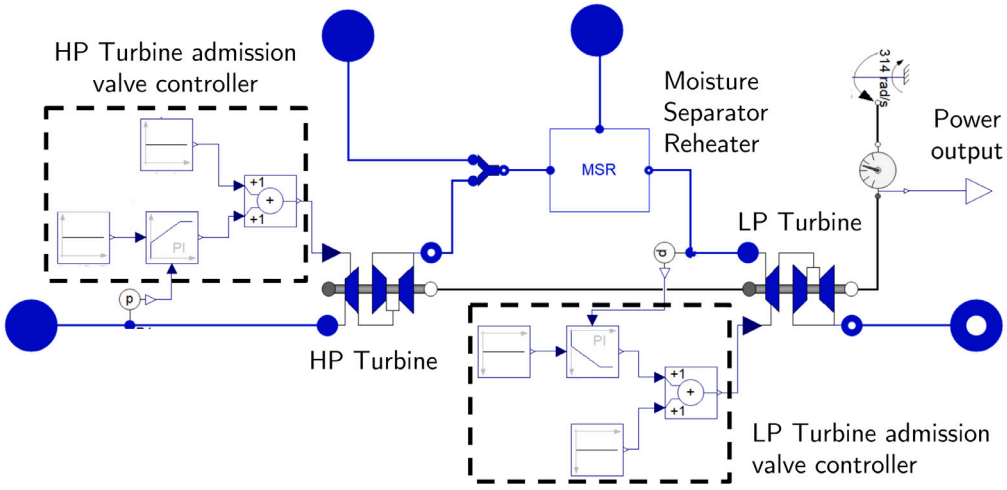

Fig. 5. Dynamic model of the balance of plant.

the pump, and the feedwater heaters, is not included in the model. This strong simplifying assumption is expected to have an impact on the dynamic analysis requirements of NHES architectures. For example, these systems may be designed to meet the variability of load demand by diverting thermal power flows to end-user applications other than electrical power production. Consequently, steam extractions within the BOP can exhibit significant variations throughout operation. These fluctuations introduce severe transients in the steam cycle, which must be thoroughly evaluated when studying the dynamics of the system. While the BOP model proposed in this study provides valuable insights regarding the electrical power produced based on a given steam input, it does not account for the dynamic behavior of the steam cycle.

Fig. 5 displays the implementation of the power conversion system in Modelica. The model relies on components of the ThermoPower library; as far as the MSR is concerned, the moisture separator is modeled by modifying the ThermoPower `DrumEquilibrium` component by adding an additional interface for the drained liquid. This component is governed by energy and mass balance equations, which are modified as follows:

$$\begin{aligned} \frac{dM}{dt} &= \dot{m}_{\text{feed}} - \dot{m}_{\text{steam}} - \dot{m}_{\text{drain}} \\ \frac{dE}{dt} &= \dot{m}_{\text{feed}} h_{\text{feed}} - \dot{m}_{\text{steam}} h_{\text{steam}} - \dot{m}_{\text{drain}} h_{\text{drain}} \end{aligned} \tag{1}$$

where the separated liquid flow rate is given by:

$$\dot{m}_{\text{drain}} = \dot{m}_{\text{feed}}(1-x)\eta_{\text{MS}} \tag{2}$$

For the reheater, the same model structure employed for the steam generator is used. The `SteamTurbineUnit` component from the ThermoPower library has been chosen to model the HP and LP turbine stages. As shown in Fig. 5, a mechanical connector is employed to link the shafts of these stages and to impose the rotational speed as a boundary condition. Furthermore, the primary governing equations for ThermoPower's `SteamTurbineUnit` are outlined in Appendix A. This simplified turbine model is unable to capture the dynamics of the machine during severe off-design conditions resulting from steam extraction. However, for the scope of this work, the model effectively fulfills the requirements of the BOP model by estimating the electrical power output of the system.

The BOP model is linked with the other NHES models through three inlet flanges, representing the flow entering the HP turbine stage, the flow entering the hot side of the reheater, and an additional flange that considers an additional mass flow contribution joining the flow at the HP turbine outlet. The input parameters required for both turbine stages and the MSR were determined by adapting the data available for the IRIS BOP to be in line with the E-SMR's operating conditions and are reported in Table 3.

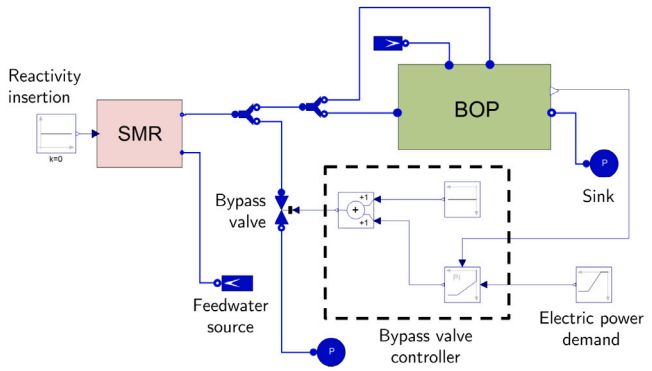

Fig. 6. System layout for load following by cogeneration.

As described in Appendix B, a decentralized control scheme based on single-input, single-output PID (proportional–integral–derivative) controllers is used to avoid pressure fluctuations at the inlet of the two turbine stages. These components regulate the turbine admission valves so that the inlet pressures remain at their nominal values even when the steam mass flow entering the turbine changes. Specifically, `SteamTurbineUnit` model operates under a partial arc admission strategy rather than throttling [44], thereby reducing thermodynamic losses driven by pressure drops in the throttling valves. Due to the turbine's pressure ratio being higher than the critical ratio of about 0.5, the model relies on the assumption of choked flow conditions [45]. Consequently, the mass flow rate can be regarded as being approximately proportional to the inlet pressure without being affected by the outlet pressure. In the considered control scheme, the turbine admission valve regulates the proportionality constant between the latter variables, as shown in the governing equations collected in Table A.7.

By employing this control strategy, significant variations in the steam generator pressure are avoided. Such fluctuations would otherwise lead to alterations in the thermodynamic state of the secondary coolant and subsequently impact its heat removal capabilities. As a result, the primary coolant conditions and the overall state of the reactor would be affected. However, it is important to note that this control strategy maintains a constant pressure ratio for the turbines, even during off-design conditions with reduced mass flow. Such operations might not comply with the constraints specified by the steam turbine manufacturer. Therefore, it will be relevant to explore alternative control strategies capable of effectively managing high steam extractions with a comprehensive BOP model.

Fig. 6 shows a possible configuration in which the SMR model is connected to the power conversion system through the dedicated interfaces. In particular, the layout displayed in Fig. 6 allows the reactor to be operated in the load following by cogeneration mode: by introducing a bypass valve at the turbine inlet, it is possible to regulate the electric output of the system to meet a certain load demand by diverting a portion of the steam driving the turbine through the bypass valve. A PID controller is also used in this case to regulate the bypass valve opening so that the turbine's electrical output matches the load demand. This architecture will be the core of the NHES layouts that will be presented in the following sections, since in every case study the SMR is operated in load following by cogeneration, employing the bypassed steam for energy storage charging or, in general, to drive cogeneration processes.

Operating a reactor in load following by cogeneration mode, which involves meeting variable load demands while maintaining the reactor at its rated power level and utilizing excess power for the production of additional commodities, offers several technical and economic benefits. This strategy combines the advantages of operating the reactor in baseload mode with the capability of providing flexibility to the electrical grid, making it an attractive option to cope with the intermittency of renewables and improve the economic competitiveness of nuclear energy. From an economic standpoint, steady operation at nominal conditions is generally preferred as the reactor's operational expenses are primarily associated with fixed costs rather than marginal costs. Moreover, flexible operation (i.e., modulation of thermal power production) increases the stresses on the reactor's components, leading to increased wear and tear and less effective fuel usage. As the penetration of VREs in the energy system continues to increase, the flexible operation of nuclear power plants will become crucial to ensuring grid stability. Load following by cogeneration mode may offer a viable approach to achieving this while also benefiting from the streamlined operational procedures that characterize baseload operational modes and low plant-level variations in operating conditions [46].

The simulation results in terms of thermal and electrical power testing the system with a 10% load demand reduction are shown in Figs. 7(a) and 7(b). In line with the fundamental principle of the load following by cogeneration mode, the thermal power of the SMR remains at its rated level throughout the whole transient, while the electric power output is reduced by 10% acting on the steam flow rate flowing through the valve. Moreover, although a significant mass flow rate is bypassed, as depicted in Fig. 7(c), Fig. 7(d) demonstrates that by regulating the admission valves of the turbine, the inlet pressures are effectively maintained at their nominal values.

4.3. Thermal energy storage system

As mentioned in Section 3.2, a two-tank sensible heat storage system employing Therminol-66 as a storage medium was considered for the energy storage technology in the NHES.

Several options are available for integrating a TES unit with a nuclear power plant. This study focuses on a configuration where the TES is charged with steam extracted at the HP turbine stage inlet. Regarding the steam produced by the TES during the discharging process, two distinct cases are considered in this work. The first case involves delivering the steam to an industrial facility, while in the second case, the steam is used to increase the electrical power output of the system. It is worth mentioning that various integration options are available for the latter application [47]. For instance, the produced steam can either be fed to the BOP or employed to drive a dedicated turbine. These approaches need to be evaluated from different standpoints, including technical feasibility, impact on system efficiency, and overall economic implications. In the proposed case study, the steam is injected into the LP turbine stage. Consequently, the LP turbine must be oversized compared to the scenario where the discharged steam is utilized solely for industrial end-user processes, resulting in higher costs and technical challenges due to the repeated off-design operations.

The configuration in Fig. 8 is used as a reference for the dynamic modeling in Modelica. In the charging process, the bypass valve diverts a part of the steam produced by the SMR towards an intermediate heat exchanger (IHX). Here, the thermal power is transferred to the sensible medium that is flowing from the cold tank to the hot tank through the IHX. In order to recover the stored energy, the heat discharged by the Therminol-66 flowing from the hot tank to the cold tank is used to produce steam in a Once-Through Steam Generator (OTSG). In both processes, the oil flow rates are regulated by pumps so that the tanks' temperatures remain at nominal levels, i.e., 205 °C for the cold tank and 260 °C for the hot tank, throughout the whole operation [12]. The steam produced in the OTSG enters a steam dome, where any liquid droplets entrained in the steam flow are removed. Finally, the steam can be used for various applications, depending on how the TES is integrated into the NHES. For example, in the scheme in Fig. 8, the energy storage system is used to perform electrical peaking, i.e., inject additional steam in the LP turbine stage to increase the electrical output of the system beyond its rated power [12].

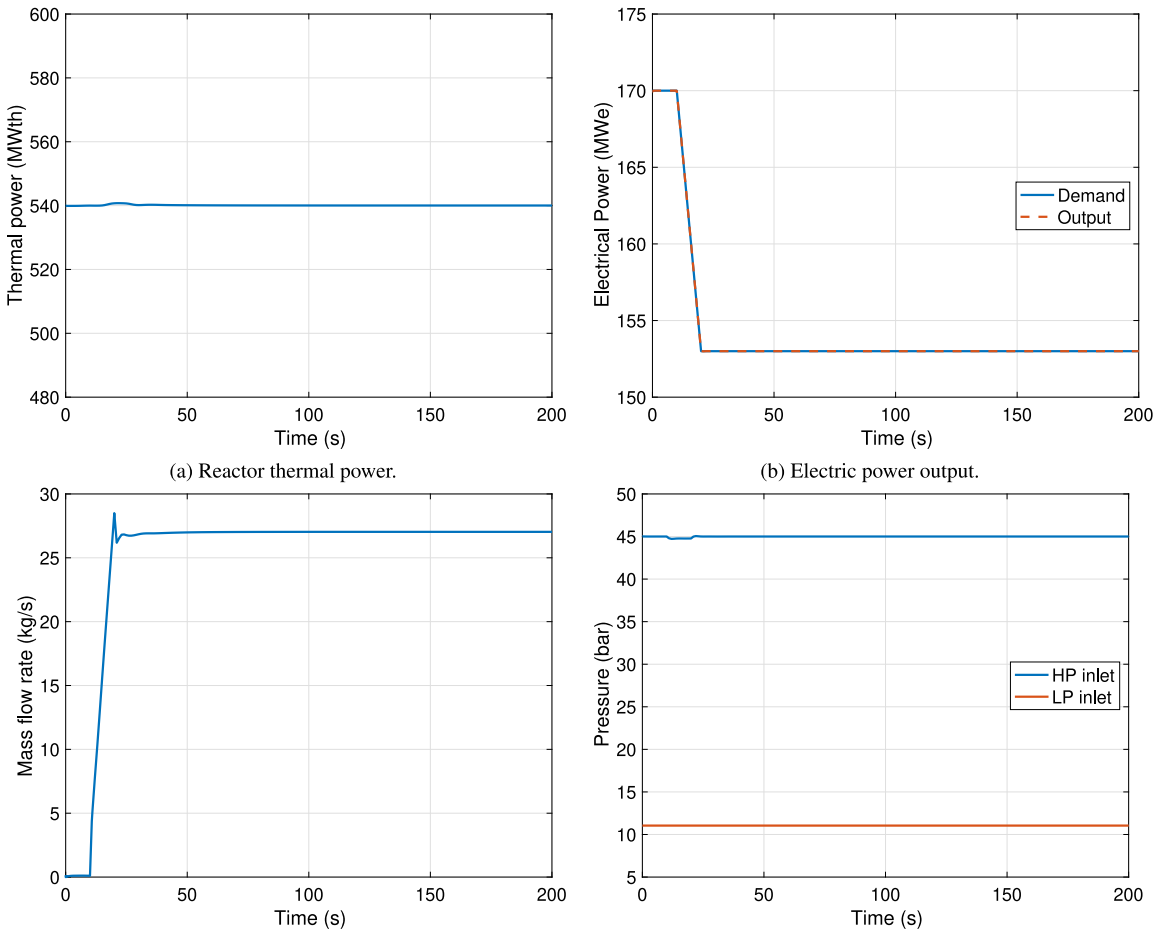

(a) Reactor thermal power.

(b) Electric power output.

(c) Bypass steam flow rate.

(d) Turbine stages inlet pressures.

Fig. 7. Simulation results with 10% load reduction.

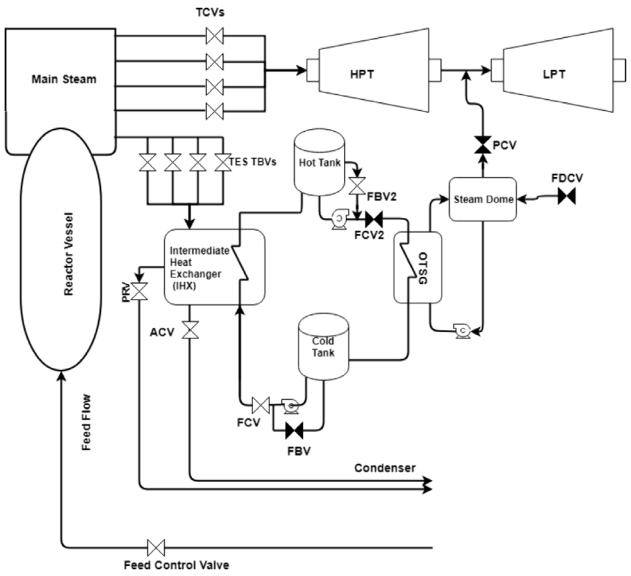

Fig. 8. Two-tanks sensible heat storage system [12].

The following submodules were developed independently and then connected to obtain the overall TES model: the IHX, the OTSG, the sensible fluid loop, and the steam dome. For the IHX and the OTSG, which are both shell-and-tube heat exchangers, the same modeling strategy applied for the steam generator, shown in Fig. 3, was adopted. In this case, the IHX model was further simplified by assuming that the steam leaves the IHX as saturated liquid. In the OTSG, the Kandlikar correlation was employed to model the evaporation process.

The sensible fluid loop model is displayed in Fig. 9. Since Therminol-66 is not included neither in the ThermoPower library nor in the Modelica Standard Library, it had to be defined as a new fluid, specifying also the correlations to compute its thermophysical properties. The sensible medium loop model includes the cold and hot tanks, as well as two ThermoPower library components that allow the synthetic oil flow rate to be imposed, eliminating the need to model pumps in the sensible fluid loop. The tanks have been modeled simplifying ThermoPower's water-gas accumulator component by removing the contribution of the gas to the model and by replacing the water fluid model with the one for Therminol-66. Consequently, the mass and energy balance equations have been adapted as presented in Appendix A.

It is worth noting that, as a first approximation, the pressure distribution within the tanks is considered to be uniform, and heat dispersion to the environment is neglected, even though the latter may be considerable if a thermal insulation is not properly provided. These simplifications are justified as the proposed TES model, meant as a preliminary representation, does not aim to provide an accurate description of the system dynamics but rather to showcase the strategy for integrating an energy storage system into different NHES architectures.

Four flanges serve as an interface between the sensible fluid loop and the IHX and OTSG, where Therminol-66 flows in the heat exchangers' tube sides. Finally, the steam dome was modeled using the moisture separator model, considering that these components have essentially the same function.

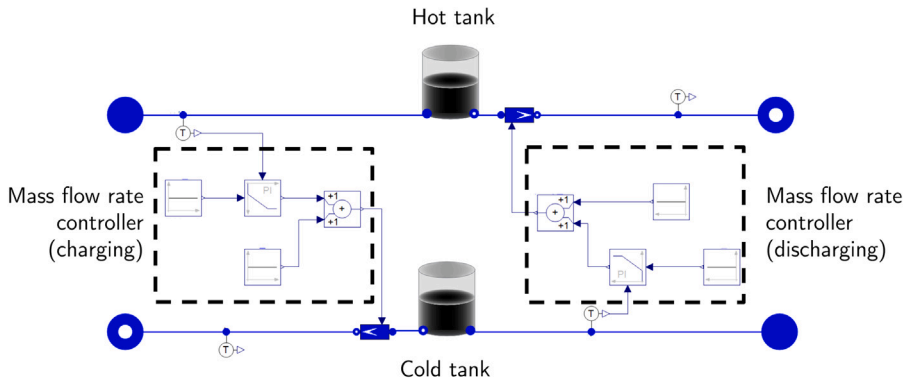

Fig. 9. Dynamic model of the sensible medium loop.

As shown in Fig. 9, a control strategy based on PID was used to regulate the oil flow rate through the heat exchangers in order to keep the tanks' temperatures at their nominal value. In addition, a controller was employed to determine the feedwater flow rate entering the OTSG to satisfy a certain steam demand.

The model's prediction capabilities were assessed by comparing the simulation results with those obtained with a reference model included in the HYBRID repository, which comprises a Modelica-based library developed in the framework of the aforementioned Integrated Energy System program [48]. The validation was performed as follows: the parameters of the TES model proposed in this work were updated to be the same as those of the reference case study, and the response of the system was tested by imposing the same input variables, i.e., bypass steam flow rate and steam demand. Lastly, the simulation outcomes of the two models were compared in terms of sensible fluid flow rates both in the charging and discharging phases, as well as tank temperatures and discharged steam flow rate. Fig. 10 shows the comparison between the Therminol-66 flow rates. The charging flow rate increases with the bypass steam flow rate due to the higher amount of thermal power transferred to the storage system, while the flow rate from the hot tank to the cold tank is determined by the steam flow rate released from the TES. In both processes, the sensible fluid flow rate is regulated to keep the temperatures between the two tanks at their nominal values. In general, the results obtained with the model exhibit good agreement with the reference profiles, except in the first part of the charging process: the flow rate predicted by the model is essentially proportional to the bypass steam flow rate, while the reference curve reaches a plateau. This is due to the fact that the flow rate in the latter instance is regulated by a valve that limits the flow rate according to its maximal opening. Moreover, the computed mass flow rates proved to be in agreement with the operational constraints of the system, i.e., the tank temperatures were kept at their nominal level and the steam demand was met during the whole charging process.

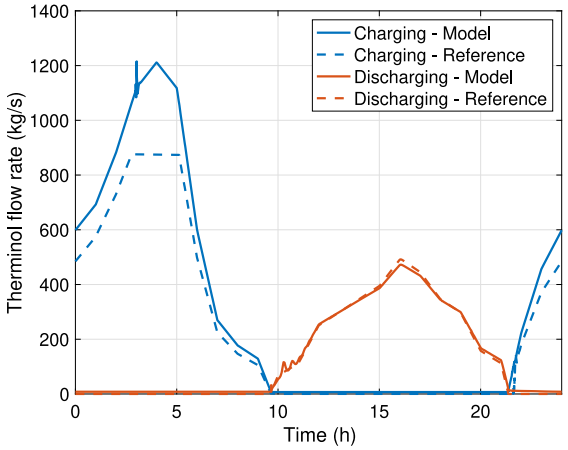

Fig. 10. Response of the TES model compared to a reference model [12].

4.4. Alkaline electrolyzer

The main objective of the alkaline electrolyzer model is to estimate the amount of hydrogen that can be produced with a certain input of electric power. To achieve this goal, as a first approximation, just the electrolyzer stack was modeled, neglecting all the other components required in a hydrogen production plant, such as the gas separators, the hydrogen storage tanks, etc. These components form the plant BOP, which is essential to capturing the dynamics of the system. As the proposed model does not encompass this part of the hydrogen production plant, it should be regarded as a preliminary tool and does not aim to offer any insights into the dynamic behavior of the overall plant.

A multi-physics model based on the work proposed by Hammoudi et al. [49] was implemented in Modelica to simulate the electrochemical, thermodynamic, geometrical, and two-phase flow phenomena occurring in the electrolyzer cell. This model allows computing overpotentials related to partial electrode coverage by gas bubbles, in addition to ohmic and activation overpotentials:

$$v = v_{\text{rev}} + v^{c}_{\text{act}} + v^{a}_{\text{act}} + v^{c}_{\text{bub}} + v^{a}_{\text{bub}} + v_{\text{ohm}} \tag{3}$$

These will contribute to the estimation of the potential difference between the electrodes. This variable, together with the electric power that drives the electrolyzer, allows computing the current flowing in the electrolyzer, which in turn is proportional to the amount of hydrogen produced.

The reference configuration taken in the latter study, which is also adopted in this work, is that of the alkaline electrolyzer developed by the Hydrogen Research Institute, whose single stack has a rated power of 5 kW [49].

The resulting I-V curve, together with a comparison with the reference model [49], is shown in Fig. 11. Due to the different modeling assumptions, e.g., the use of a constant electrical conductivity for the electrode materials, the model overestimates the cell potential; however, the outcomes are considered sufficiently accurate for the purposes of the simulator.

5. NHES architectures

In a broad framework for the analysis of NHES, it is fundamental to be able to easily assemble multiple NHES architectures starting from the individual technologies collected in the new Modelica library. In this way, it is possible to simulate the dynamic behavior of a large number of configurations, enabling the comparison of their performances according to the boundary conditions.

Table 4
Overview of the considered NHES architectures.

Architecture	Interconnections	Commodities
H_2 supply	Electrical	Electricity, hydrogen
TES for process steam supply		
Process steam supply	Electrical, thermal	Electricity, process steam
Combined process steam — H_2 supply	Electrical, thermal	Electricity, process steam, hydrogen
TES for electrical peaking		
Electrical peaking	Electrical, thermal	Electricity
Combined peaking — H_2 supply	Electrical, thermal	Electricity, hydrogen

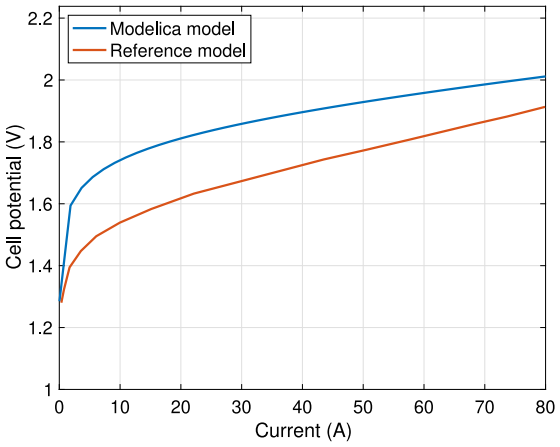

Fig. 11. I-V of the developed model compared to the reference model [49].

As aforementioned, the optimal NHES architecture resulting from this analysis will be strongly dependent on the operational context. For example, if the local energy mix features a large penetration of VREs, it is reasonable to assume that the energy storage capacity of the most suitable NHES layout will be higher in order to provide a higher degree of flexibility to the electrical grid.

The following sections provide a description of the NHES architectures obtained by combining the LW-SMR, the thermal energy storage system, and the hydrogen production unit. The resulting architectures, together with the types of interconnections and the commodities produced, are summarized in Table 4.

5.1. Industrial process steam supply

In this first architecture, the thermal energy storage system is coupled to the SMR and is used to deliver process steam to an industrial facility. The amount of steam as well as its thermodynamic state depend on the requirements provided by the industrial facility itself. In this work, the steam production capability of the system is tested by imposing the conditions of a real-world example of nuclear cogeneration for process steam production. The case of the Gösgen nuclear power plant, in Switzerland, where 22 kg/s of steam at 13.7 bar and 220 °C are supplied to a cardboard factory, is considered for reference [10]. Throughout the 24-hour period, the steam demand is assumed to remain constant.

The model in Modelica expands upon the fundamental design presented in Fig. 6. In this NHES, the steam extracted via the bypass valve is diverted to the TES unit and drives the charging process. On the other hand, the steam produced in the discharging process is delivered to the industrial facility, represented by a flow sink. In addition to the control system described in Section 4, meant to regulate the bypass valve opening according to load demand, an additional control scheme to determine the OTSG feedwater flow rate to meet the required process steam conditions is also included.

5.2. Hydrogen supply

Integrating only the low-temperature electrolysis hydrogen production unit into the NHES, the system features only electrical interconnections, i.e., the steam produced by the SMR is entirely fed into the turbine to be converted into electricity.

In this configuration, load demand is met by converting the whole excess electricity into hydrogen through water electrolysis. To accomplish this, the number of stacks required to handle the maximum difference between the electrolyzer's rated power and the load demand over a 24-hour period must be determined. It is important to note that alkaline electrolyzers can be operated in a range limited to 15%–100% of their rated power [50]. In other words, a constraint that must be taken into account while assessing the optimal operation mode of the NHES is that the electrolyzer should always be supplied with a minimum amount of electricity.

In the dynamic model of this configuration, the SMR is linked with the power conversion system, eliminating the need to include the bypass valve and its related control system. Furthermore, a simplified control strategy is introduced to compute the excess power to be delivered to the electrolyzer and ensure that the least amount of power is fed to the hydrogen production unit.

5.3. Combined process steam and hydrogen supply

The NHES described in this section, whose implementation in Modelica is depicted in Fig. 12, is composed of the SMR, the energy storage system, as well as the hydrogen production unit. In this case, the steam produced by the TES is also delivered to the industrial processes. In this configuration, the excess energy can be allocated either to the storage system or to the electrolyzer. This allows for the reduction of the hydrogen production capacity with respect to the previous architecture, decreasing the required capital costs, for example. Therefore, the electrolyzer size is assumed to be limited to 10% of the NHES rated power, i.e., 17 MW.

At this point, it is necessary to introduce a dispatch strategy to be able to allocate the energy flows in the NHES to the various subsystems. In a comprehensive framework, the dispatch strategy will result from a techno-economic optimization of the NHES operation. Since this kind of analysis goes beyond the scope of this study, the energy dispatch strategy is defined in advance. In particular, priority is given to meeting a certain load demand. If excess power is available, it is first allocated for hydrogen production. When it is higher than the electrolyzer capacity, the charging process is activated, i.e., the electric power output is reduced by modulating the opening of the bypass valve.

5.4. Electrical peaking

In this architecture, the service provided by the thermal energy storage system is electrical peaking, i.e., the stored energy is employed to produce additional electricity to satisfy load demand peaks. Fig. 8 depicts the TES integration scheme into the NHES: the steam produced during the discharging process is fed into the LP turbine stage to increase the system's electrical output beyond its rated power. As a

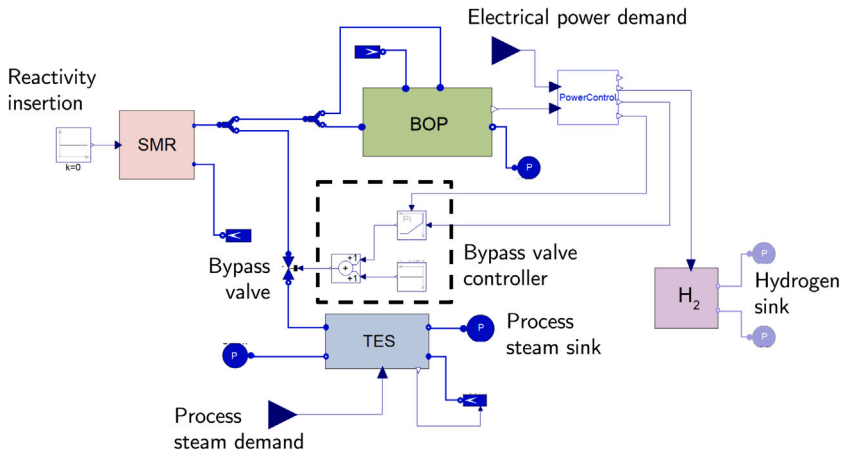

Fig. 12. Combined process steam and hydrogen supply architecture.

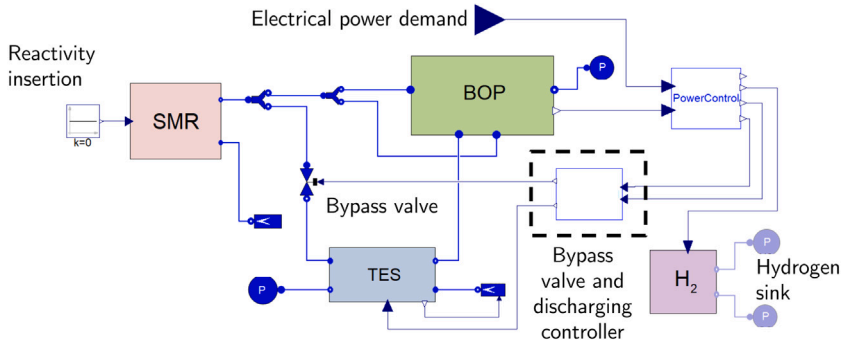

Fig. 13. Combined electrical peaking and hydrogen supply architecture.

result, the size of the LP turbine stage must be altered in comparison to previous architectures, as it must be able to cope with a larger steam flow rate than the nominal level. Of course, installing a turbine characterized by a higher rated power output has economic implications that must be considered in the evaluation of the profitability of this NHES layout. It is worth emphasizing that no additional commodities are produced with this architecture, meaning that the NHES has access only to the electricity market.

The control strategy applied to this design builds on the one described for the earlier cases by introducing logic signals to activate either the charging process, by regulating the bypass valve opening when load demand is lower than the nominal power, or the discharging process, by injecting additional steam into the power conversion system and meeting demand peaks. This system is necessary to prevent the TES from being charged and discharged at the same time, e.g., by meeting a certain load demand by reducing the mass flow rate through the bypass valve and simultaneously providing additional steam to the LP turbine.

5.5. Combined electrical peaking and hydrogen supply

The latter layout is extended to include the electrolyzer in the NHES. As a result, the system, represented by the model displayed in Fig. 13, will produce hydrogen as an additional commodity.

For this configuration as well, the dispatch strategy needs to be defined in advance. Similarly to the energy dispatch presented in Section 5.3, priority is given to meeting load demand while the excess power is diverted for hydrogen production up to the electrolyzer's maximal capacity and then used for TES charging. During the electrical peaking period, power is delivered both to the electrical grid and to the electrolyzer, which is operated at its minimal level.

5.6. Control strategies

The control strategies mentioned in the previous sections have been summarized in Table 5. Overall, the purpose of the control schemes is to adjust the controlled variable to meet demands, in this case in terms of load and process steam, as well as to ensure that the NHES operation complies with the system's technical constraints, such as maintaining operating pressures at nominal values.

The table provides an overview of the control systems for different energy products; as described above, NHES architectures may combine multiple subsystems, e.g., they might encompass process steam supply or electrical peaking with hydrogen production, as discussed in Section 5.3 and Section 5.5, respectively. Logical signals, which are triggered when the controlled variables reach a given threshold, and PIDs are included in the control strategies. The latter control components were calibrated adopting a decentralized control scheme, meaning that each controlled variable is regulated by a single process variable.

If the NHES architecture combines two of the energy outputs listed in the table, e.g., process steam supply and hydrogen production, the overall control strategy is obtained by merging the corresponding columns. For instance, in the latter NHES architecture, the electrical power output will be regulated by employing a fraction of the excess electrical power for hydrogen production and by controlling the bypassed mass flow rate.

6. Scenarios

The five NHES architectures were tested with different boundary conditions in terms of load demand over a 24-hour period. As discussed in Section 2, these scenarios are just meant to evaluate the response of

Table 5
Overview of the control strategies employed in the NHES architectures.

Process variable	Controlled variable	Control strategies for different cogeneration options		
		H_2	Process steam	Electrical peaking
SMR pressure	Sprayers, heater	Logical	Logical	Logical
Turbine inlet pressure	Admission valves opening	PID	PID	PID
Tank temperatures	Sensible fluid flow	–	PID	PID
Process steam flow	TES feedwater flow	–	PID	–
Electrolyzer power	Excess electrical power	Logical	–	–
Electrolyzer temperature	Electrolyte flow	PID	–	–
	Bypass valve opening	–	PID	PID, logical (charging)
Electrical power output	TES feedwater flow	–	–	PID, logical (discharging)
	Excess electrical power	Logical	–	–

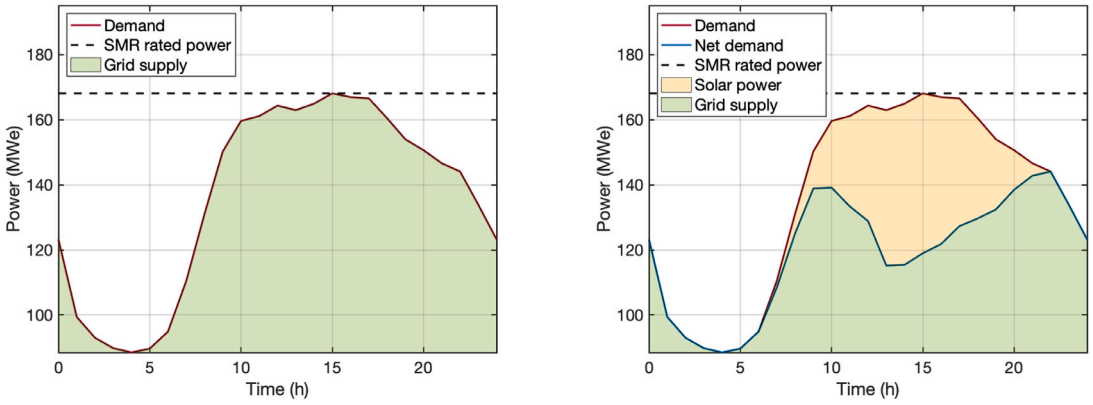

(a) Baseline scenario.

(b) High PV penetration scenario.

Fig. 14. Scenarios considered to test the NHES architectures.

the system. In the context of NHES analysis, employing faithful models for this assessment can offer valuable insights into the system ability to provide flexibility to the grid. For instance, it enables verifying whether the configuration can effectively allocate energy flows to cope with varying loads and meet ramping-up requirements by comparing the results with the constraints on ramping rates of the considered components. The two scenarios considered in this work are shown in Fig. 14. The reference load profile is that of a typical summer day [51]: it features a rapid ramp-up in the morning, due to the activation of household and industrial appliances, before reaching a peak in the afternoon.

The reference demand was rescaled to be in compliance with the power output that can be actually provided by the NHES architectures, which differs according to the service provided by the thermal storage unit. When it is used to supply process steam to the industrial facility, the electric power output is limited to the SMR's rated power, i.e., 170 MWe. On the other hand, a different rescaling factor must be used when the TES allows for meeting higher demand peaks; in this case, the maximal power output is set 20% higher than the rated power of the system.

The second scenario aims to account for a significantly higher penetration of VREs, in particular solar power. The net load profile is obtained by subtracting the solar power output, which is proportional to both a factor accounting for the installed capacity of solar PVs and the Direct Normal Irradiation (DNI) to consider the variability of solar intensity throughout the 24-hour period.

It is important to note that, despite these time series stemming from real load profiles, these conceptual scenarios are intended just to test the dynamic behavior of the system and are not meant to represent a real-life situation, since the actual flexibility requirements of the NHES depend on the share of all generators in the local energy mix and its projected future evolution.

7. Results

The simulation outcomes obtained by testing the proposed NHES architectures with the aforementioned scenarios are presented in this section. Table 6 collects the energy allocated to each NHES component in the two case studies. The values were obtained by integrating the power flows over the whole period of interest, i.e., 24 h. This kind of outcome might be useful for an economic evaluation of the NHES architectures, since revenue streams can be associated with each energy product. To provide a basis for comparison, the table includes a scenario where the load demand is met through conventional load following, i.e., by regulating the thermal power output of the reactor by means of control rods. The resulting SMR power was obtained by adjusting the electric power output with the thermal efficiency of the SMR, assumed to be 31.48%. It is worth mentioning that the thermal energy produced by the SMR is the same in each case study considered in this work. This is related to the fact that the reactor is operated in load following by cogeneration, so the thermal power output remains steadily at its nominal value in each transient. On the other hand, this variable is considerably lower in the case of conventional load following, especially in the high PV scenario, implying that the reactor may experience the aforementioned drawbacks related to its flexible operation.

The electrical energy supplied to the grid in the baseline scenario appears to be different in the first three configurations, despite the fact that the load profile is the same. According to this finding, the load demand in some case studies may not be fully met. This occurs due to the constraint of minimal electrolyzer power: when the hydrogen production unit is coupled to the system, a portion of the electric power output must be allocated to this subsystem, so the remaining part might not be sufficient to meet load demand. This is not the case in the high PV scenario, where net grid demand is significantly lower due to the contribution of solar power. As far as the grid, steam, and

Table 6
Energy dispatch for the two scenarios.

Architecture	SMR (GWh_{th})	Charging (GWh_{th})	Grid (GWh_{el})	Steam (GWh_{th})	Hydrogen (GWh_{H2})	Efficiency (%)
Baseline scenario						
Conventional load following	10.74	–	3.38	–	–	31.5
H_2 supply	12.96	–	3.22	–	0.59	29.4
Process steam supply	12.96	2.27	3.38	1.08	–	34.4
Combined process steam — H_2 supply	12.96	1.45	3.27	1.08	0.2	35.1
Electrical peaking	12.96	1.35	3.93	–	–	30.3
Combined electrical peaking — H_2 supply	12.96	0.91	3.93	–	0.13	31.3
High PV scenario						
Conventional load following	9.15	–	2.88	–	–	31.5
H_2 supply	12.96	–	2.88	–	0.82	28.5
Process steam supply	12.96	3.41	2.88	1.08	–	30.6
Combined process steam — H_2 supply	12.96	2.26	2.88	1.08	0.27	32.6
Electrical peaking	12.96	1.93	3.45	–	–	26.6
Combined electrical peaking — H_2 supply	12.96	1.06	3.45	–	0.21	28.2

hydrogen are concerned, the energy embedded in these commodities is considered to account for the downstream energy product. For this reason, energy related to hydrogen is not computed with the electric power flows allocated to the electrolyzer but by multiplying the amount of hydrogen produced by its lower heating value. In this way, it is also possible to account for the electrolyzer's efficiency. The efficiencies of each configuration in the two scenarios are determined based on the total energy output, which includes the energy supplied to the grid as well as the energy generated in the form of process steam and hydrogen, relative to the thermal energy supplied by the SMR. In the baseline scenario, the only configurations that feature a higher efficiency compared to conventional load following are those in which process steam is supplied as an additional commodity. This can be attributed to the fact that the thermal energy generated by the reactor is initially stored in the TES unit and then discharged directly as thermal power, foregoing energy transformations that would result in inevitable losses. Power conversion occurs when the energy produced by the reactor is converted into electricity and, subsequently, hydrogen. When the TES is integrated as an electrical peaking unit, the system experiences a loss in efficiency, suggesting that the intermediate storage process introduces additional losses, which might be eventually reduced by exploring different TES integration options. It is worth noting that the power allocated for TES charging is not considered when calculating the system efficiency since it is not regarded as a valuable energy output of the system. Consequently, case studies with higher thermal power diverted to the TES, particularly in the high PV scenario, exhibit lower efficiency. Overall, the computed values are affected by the assumptions adopted for the implementation of the model, such as the "open cycle" hypothesis applied to the BOP. A more representative model might change the dynamics of the system and thus the energy dispatched between the subsystems.

The following sections summarize the results obtained in the configurations comprising the three technologies presented in this work, namely, the layouts in which the SMR is coupled to the thermal energy storage system, used for process steam supply or electrical peaking, and the hydrogen production unit, as representative examples of simulation outcomes.

7.1. Combined process steam and hydrogen supply

The simulation outcomes presented in this section were obtained by testing the configuration depicted in Fig. 12 and described in Section 5.3. In this particular setup, hydrogen is produced as an additional commodity, and the TES unit is employed to supply process steam to an industrial facility.

The system response in the baseline scenario is illustrated in Figs. 15(a) and 15(b). Fig. 15(a) displays how the reactor's thermal power, which remains constant at the nominal value of 540 MWth, is distributed among the storage system and the BOP according to load demand. Additionally, throughout the 24-hour period, a constant contribution increases the thermal power output of the system, which is related to the continuous supply of industrial process steam produced by the thermal power released by the TES. It is important to note that in this application, thermal power is not converted into electricity; hence, the latter contribution is not present in Fig. 15(b). The electrical power flows in Fig. 15(b) reveal that a portion of energy is converted into hydrogen. However, it can be observed that the load demand is not satisfied when it reaches its peak due to the minimal power required by the electrolyzer. This outcome is strongly dependent on the dispatch strategy, the NHES layout, and its operation strategy. For example, this issue could be overcome by operating the electrolyzer in hot standby during this period, i.e., keeping the device at its operational temperature but without powering it.

Similar observations can be made in the high PV scenario, for which the thermal and electrical power flows are depicted in Figs. 15(c) and 15(d), respectively. In contrast to the previous scenario, the significantly lower load demand compared to the rated power enables the electrolyzer to operate steadily at full capacity. This finding suggests that, in contexts where load demand is low, increasing the electrolyzer's capacity could be advantageous in order to convert the excess power into a valuable product, such as hydrogen or process steam, rather than storing it in the TES unit.

It is worth noting that the TES state of charge at the end of the transient does not always correspond with the initial charge, as the level of power input and output is determined by the operating requirements in the examined scenarios. Specifically, the power flows in Fig. 15 and the values for charged energy and steam energy in Table 6 demonstrate that the level of energy stored in the TES is much higher than that discharged from the storage system.

7.2. Combined electrical peaking and hydrogen supply

In the second NHES configuration, described in Section 5.5, the TES unit is used to enhance the flexibility of electrical power production and increase the overall power output of the system. In this setup, TES discharging is triggered when the load demand exceeds the rated power. As aforementioned, in this case study the load demand that needs to be satisfied by the NHES is increased to reach an electrical peak that is 20% higher than the nominal power in order to fully appreciate the discharge process.

The simulation results for the baseline scenario, depicted in Figs. 16(a) and 16(b), show that a significant amount of thermal energy is released during the discharging process to increase the electrical power output. However, the achieved thermal efficiency, computed as the ratio of energy delivered to the grid during the peak to the discharged thermal energy, is approximately 19%. This value is considerably lower than the steam cycle efficiency of 31.5%, suggesting that

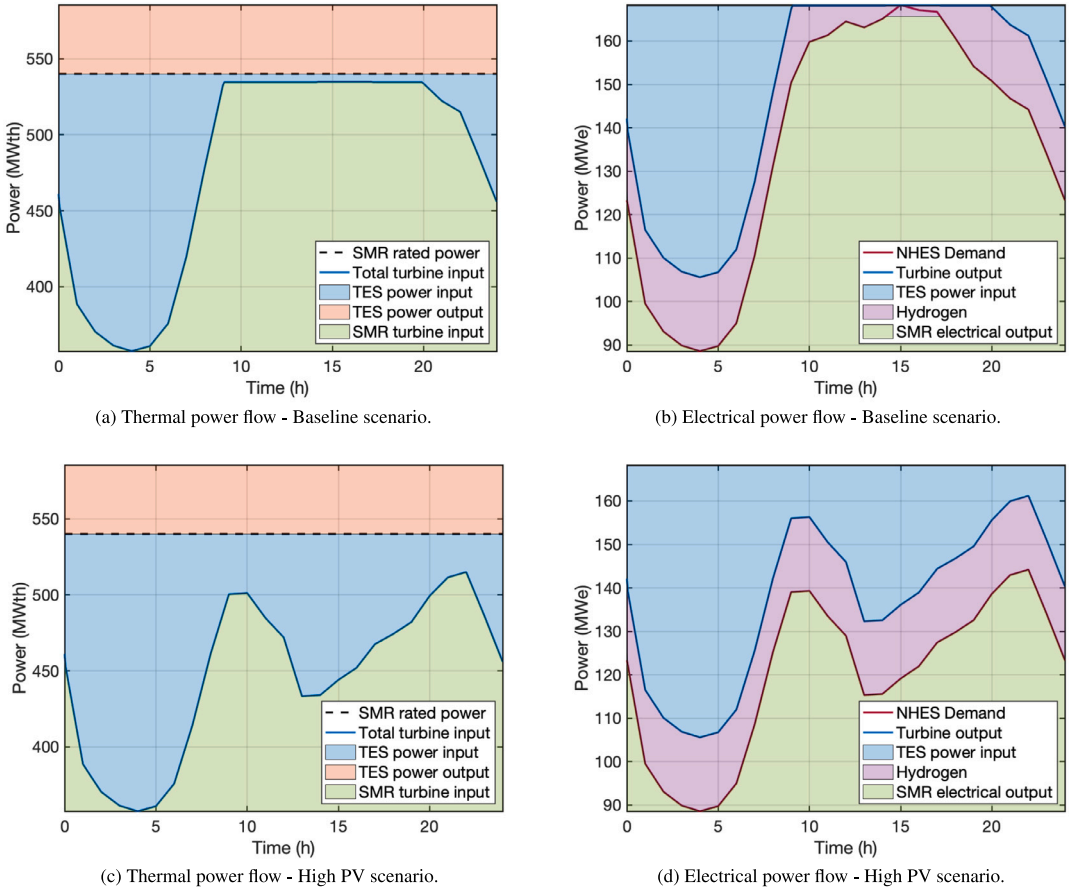

(a) Thermal power flow - Baseline scenario.

(b) Electrical power flow - Baseline scenario.

(c) Thermal power flow - High PV scenario.

(d) Electrical power flow - High PV scenario.

Fig. 15. Thermal and electrical power flows in the combined process steam and hydrogen supply architecture.

injecting additional steam into the LP turbine when electricity demand is high is not an efficient solution. Thus, it becomes worthwhile to explore alternative integration options. Additionally, Fig. 16(b) illustrates that the power allocated for driving the electrolyzer aligns with the aforementioned dispatch strategy, minimizing hydrogen production during the electrical peak and maximizing it when the load demand is low.

As shown in Figs. 16(c) and 16(d), in the high PV scenario, the peaking requirements are significantly reduced compared to the previous example, leading to a different state of charge at the end of the transient. As a result, the discharge process is activated for a short time to meet the demand peak and provide the minimum power required by the electrolyzer.

8. Conclusions

In this work, dynamic models of NHES components were developed and assembled into a variety of NHES architectures. As representative examples of candidate technologies, a LW-SMR, together with its energy conversion system, a thermal energy storage unit, and an alkaline electrolyzer, were selected. The architectures were tested by analyzing their response to different boundary conditions in terms of load and process steam demand. In particular, two different load profiles were considered in order to account for load demand whose time behavior is characterized by a different degree of penetration of variable renewable energy sources in the energy mix.

The simulation outcomes demonstrated that the dynamic models proved to be capable of meeting their goals, i.e., they allowed for the monitoring in time of the process variables, keeping track of the energy flows within the system, and implementing control strategies to govern the dynamic behavior of the system. The NHES models are used to assess the system response to variable load demands in each scenario with different flexibility requirements. The high PV scenario, in particular, features significant load fluctuations and ramping requirements, as well as a net demand that must be met by the NHES that is significantly lower, resulting in higher excess energy to be allocated to the thermal energy storage system and to the electrolyzer. For this reason, it might be convenient to increase the storage and hydrogen production capacity, which would additionally lead to an increase in the flexibility that can be provided to the grid. The preliminary analysis of the NHES architectures revealed that having process steam as a valuable commodity significantly enhances overall efficiency. Conversely, the electrical peaking configurations exhibited a loss in efficiency. This reduction can be attributed to the selected integration method of the TES unit into the NHES. To further extend the analysis, energy and exergy analyses could be conducted to explore alternative coupling strategies and identify the optimal approach for coupling TES systems into a NHES.

The simplifications employed during the development of the models must be acknowledged, as they limit the ability to effectively forecast the dynamic behavior of the entire system. This limitation is particularly evident in the case of the BOP model, where a comprehensive representation of the steam cycle is necessary to capture the impact of variable steam extraction on the transient behavior of the system. Furthermore, the absence of thorough model validation for the E-SMR and BOP models does not allow for insights into their accuracy. Hence, future validation efforts are required to ensure the reliability of models developed to simulate the dynamics of NHES components. Overall, the dynamic models proposed in this study should be viewed as preliminary tools that need to be improved both in terms of system design and modeling approach. For the first aspect, thorough sizing procedures based on technical and economic considerations should be included

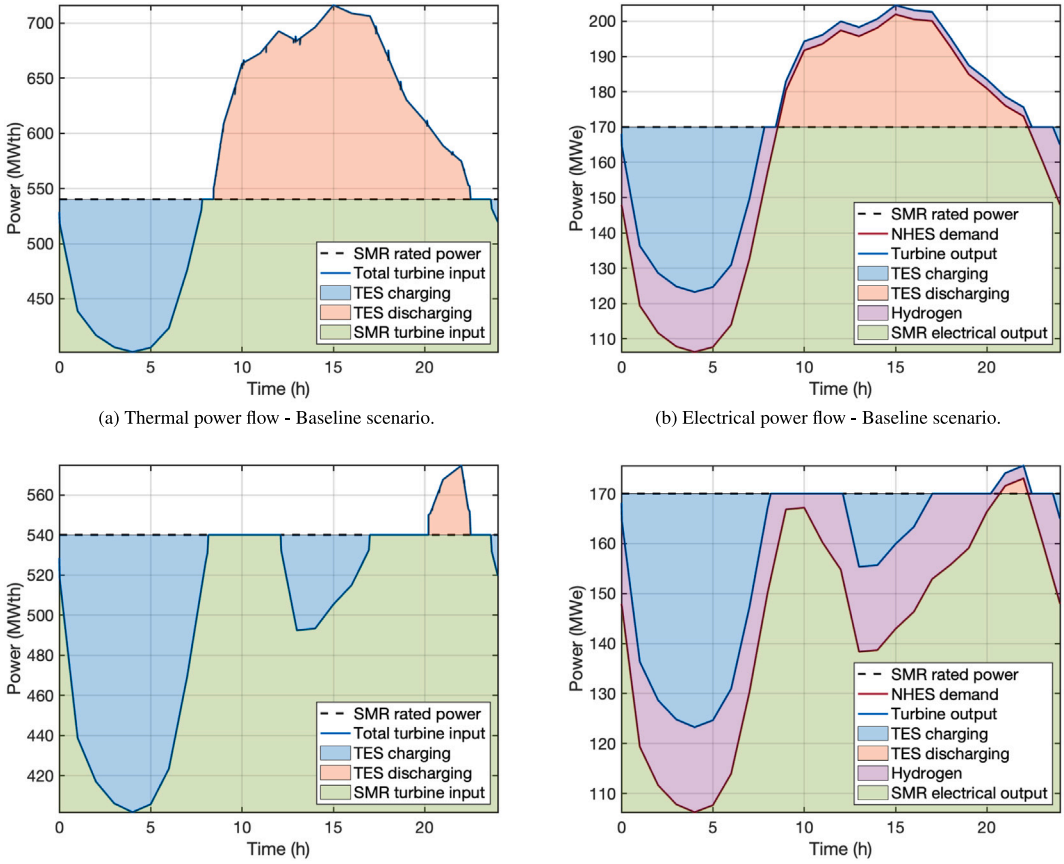

(a) Thermal power flow - Baseline scenario.

(b) Electrical power flow - Baseline scenario.

(c) Thermal power flow - High PV scenario.

(d) Electrical power flow - High PV scenario.

Fig. 16. Thermal and electrical power flows in the combined electrical peaking and hydrogen supply architecture.

for the design of the steam generator, the BOP, and the storage tanks and electrolyzer capacities. Relaxing the simplifying assumptions on which the models rely will considerably strengthen their prediction capabilities. For example, including pressure drops and primary coolant pumps in the SMR model will improve the description of the flow dynamics within the system. Moreover, the BOP model needs to be extended, including the components required to close the steam cycle model. As far as the non-electric applications are concerned, the TES should be improved by acting on the simplifying assumptions used to model the sensible medium loop, for example, while additional efforts should be dedicated to modeling the whole hydrogen production unit, and not only the electrolyzer stack, to gain a complete insight into the dynamics of the plant.

The approach proposed in this work can be seen as a first step towards the development of a wider framework for the analysis of nuclear hybrid energy systems. Modelica, as an object-oriented modeling language, proved to be particularly well suited for these applications because it allowed for simple model interchangeability. In this way, it is possible to focus on the dynamic modeling of the individual components and assemble them into many possible NHES combinations through a plug-and-play philosophy in a subsequent stage. In order to be able to build multiple NHES configurations, eventually tailoring them to the operational context, it is necessary to add more technologies, in terms of energy sources, storage systems, and electrical and non-electrical applications, to the developed Modelica library. Ultimately, the dynamic models constructed with the methodology proposed in this work should be viewed as tools to be coupled with system optimization techniques as well as thermal-hydraulic system codes to assess the overall safety of the system, for example by substituting the dynamic model of the SMR with a high-fidelity model to determine the system response in accidental scenarios. A comprehensive framework for the analysis of NHES is fundamental to being able to compare different architectures, highlight the advantages and drawbacks of this alternative with respect to other energy sources, and estimate their potential for the transition towards a sustainable energy system.

CRediT authorship contribution statement

Guido Carlo Masotti: Methodology, Software, Validation, Writing – original draft. **Antonio Cammi:** Conceptualization, Methodology, Writing – review & editing. **Stefano Lorenzi:** Conceptualization, Validation, Writing – review & editing, Supervision. **Marco Enrico Ricotti:** Conceptualization, Writing – review & editing, Project administration.

Declaration of competing interest

The authors declare that they have no known competing financial interests or personal relationships that could have appeared to influence the work reported in this paper.

Data availability

Data will be made available on request.

Appendix A. Main governing equations

See Tables A.7 and A.8.

Table A.7
Main equations of the components of the ThermoPower library and utilizations in the NHES models [25].

Component	Applications	Equations
Fluid flow (`Flow1DFV`)	Moderator flow through the core, riser, downcomer, SG, reheater, IHX, OTSG	$\frac{dM}{dt} = \dot{m}_{in} - \dot{m}_{out}$ $\frac{L}{A}\frac{d\dot{m}}{dt} + (p_{out} - p_{in}) + \Delta p_{stat} + \Delta p_{fric} = 0$ $V d\frac{dh}{dt} + \dot{m}(h_{out} - h_{in}) = \dot{Q}$
Valve (`ValveLin`)	Bypass valve, pressurizer relief valve	$\dot{m} = K_v\theta(p_{in} - p_{out})$
Fluid volumes (`Mixer`, `Header`, `DrumEquilibrium`)	Lower and upper plena, moisture separator	$\frac{dM}{dt} = \dot{m}_{in} - \dot{m}_{out}$ $\frac{dE}{dt} = \dot{m}_{in}h_{in} - \dot{m}_{out}h_{out}$
Turbine (`SteamTurbineUnit`)	HP and LP turbine stages	$\dot{m} = K_v p_{in}$, with $K_v = \theta\frac{\dot{m}_{nom}}{p_{nom}}$ $P_{mec} = \eta_{mec}\dot{m}\ (h_{in} - h_{out})$ $h_{in} - h_{out} = \eta_{iso}\ (h_{in} - h_{iso})$ $\tau\frac{dP}{dt} = P_{mec} - P$
Tube wall (`MetalTubeFV`)	SG, reheater, IHX, OTSG	$V d c_{p,w}\frac{dT_w}{dt} = \dot{Q}_{in} + \dot{Q}_{out}$

Table A.8
Main equations of the NHES subsystem components.

Component		Equations
Core [24]	Point kinetics	$\frac{dn}{dt} = \frac{\rho - \beta}{\Lambda}n + \sum_{i=1}^{8}\lambda_i c_i + q$ $\frac{dc_i}{dt} = \frac{\beta_i}{\Lambda}n - \lambda_i c_i \quad i = 1-8$
	Fuel rods	$d_f c_{p,f}\frac{\partial T_f}{\partial t} = \frac{1}{r}\frac{\partial}{\partial r}\left(rk_f\frac{\partial T_f}{\partial r}\right) + q'''$ $\frac{\partial}{\partial r}\left(rk_g\frac{\partial T_g}{\partial r}\right) = 0$ $d_{cl}c_{p,cl}\frac{\partial T_{cl}}{\partial t} = \frac{1}{r}\frac{\partial}{\partial r}\left(rk_{cl}\frac{\partial T_{cl}}{\partial r}\right)$
Pressurizer [39]	Liquid phase	$\frac{dM_l}{dt} = -\dot{m}_{\mathrm{FL}} + \dot{m}_{\mathrm{RO}} + \dot{m}_{\mathrm{SC}} + \dot{m}_{\mathrm{SP}} + \dot{m}_{\mathrm{WC}} + \dot{m}_{\mathrm{SRG}}$ $\frac{dH_l}{dt} = -\dot{m}_{\mathrm{FL}}h_v^{sat} + \dot{m}_{\mathrm{RO}}h_l^{sat} + \dot{m}_{\mathrm{SC}}h_l^{sat} + \dot{m}_{\mathrm{SP}}h_{\mathrm{SP}} + \dot{m}_{\mathrm{WC}}h_v^{sat} + \dot{m}_{\mathrm{SRG}}h_{\mathrm{SRG}} + \dot{Q}_{\mathrm{heater}} + \dot{Q}_{vl}$
	Vapor phase	$\frac{dM_v}{dt} = \dot{m}_{\mathrm{FL}} - \dot{m}_{\mathrm{RO}} - \dot{m}_{\mathrm{SC}} - \dot{m}_{\mathrm{VLV}} - \dot{m}_{\mathrm{WC}}$ $\frac{dH_v}{dt} = \dot{m}_{\mathrm{FL}}h_v^{sat} - \dot{m}_{\mathrm{RO}}h_l^{sat} - \dot{m}_{\mathrm{SC}}h_v^{sat} - \dot{m}_{\mathrm{VLV}}h_v - \dot{m}_{\mathrm{WC}}h_v^{sat} - \dot{Q}_{vl}$
TES tanks	Balance equations	$d_{\mathrm{oil}}\ \frac{dV_{\mathrm{oil}}}{dt} = \dot{m}_{\mathrm{oil}}^{\mathrm{in}} - \dot{m}_{\mathrm{oil}}^{\mathrm{out}}$ $d_{\mathrm{oil}}\ V_{\mathrm{oil}}\ \frac{dh_{\mathrm{tank}}}{dt} - p\frac{dV_{\mathrm{oil}}}{dt} = \dot{m}_{\mathrm{oil}}^{\mathrm{in}}\ (h_{\mathrm{oil}}^{\mathrm{in}} - h_{\mathrm{tank}}) - \dot{m}_{\mathrm{oil}}^{\mathrm{out}}\ (h_{\mathrm{oil}}^{\mathrm{out}} - h_{\mathrm{tank}})$
Alkaline electrolyzer [49]	Cell potential	$v = v_{\mathrm{rev}} + v_{\mathrm{act}}^{c} + v_{\mathrm{act}}^{a} + v_{\mathrm{bub}}^{c} + v_{\mathrm{bub}}^{a} + v_{\mathrm{ohm}}$

Appendix B. PID controllers

The control systems discussed in this study predominantly employ PID control algorithms, widely adopted across a broad range of industrial applications [52]. These controllers calculate the controlled variable by considering the error between the process variable and a given setpoint, according to the following equation:

$$u(t) = K_p e(t) + K_i \int e(t)\,dt + K_d\frac{de(t)}{dt} \tag{B.1}$$

where $u(t)$, is the controlled variable, $e(t)$ the error and K_p, K_i and K_d the controller parameters. The first term of Eq. (B.1) is directly proportional to the error, whereas the second and third terms account for the integral and derivative of the error, respectively. In particular, the last term becomes significant when the reference signal fluctuates at high frequencies. However, given that this is not the case in operational transients of nuclear power plants, this term was omitted in this work [53].

The gains K_p and K_i were determined using the PID Tuner application within the MATLAB Control System Toolbox. This tool provides PID gains for single-input single-output linear models, which are not applicable to the structure of the Modelica models presented in this study. Thus, a decentralized control strategy was adopted, with each PID controller independently tuned based on its corresponding process and control variable. Then, the model was linearized within the Dymola® environment and exported to the PID Tuner application.

In the context of NHES analysis, it is essential to recognize that a decentralized control strategy has several limitations. When PID controllers are tuned independently, interactions between different control loops will not be captured, which may have strong implications in highly interconnected systems like NHES. It is therefore worthwhile exploring other control approaches that may prove to be more suited for these systems.

The resulting control parameters are summarized in Table B.9. Due to the magnitude of the controlled variables, namely 10^5 Pa and 10^6 W, respectively, the pressure and power controllers show relatively small gains. On the other hand, the parameters for LP turbine admission valve controllers are substantially higher compared to those for the HP turbine, indicating faster control response. Generally, higher K_p values

Table B.9
Overview of PID controller parameters.

Controller	Process variable	Controlled variable	K_p	K_i
Balance of plant				
HP turbine admission valve	Inlet pressure	Valve opening	-7.5×10^{-8}	-4.3×10^{-7}
LP turbine admission valve	Inlet pressure	Valve opening	-8.7×10^{-3}	−2.58
Bypass valve	Electrical power	Valve opening	-5×10^{-9}	-1×10^{-9}
Thermal energy storage				
Cold-to-hot tank flow	Hot tank temperature	Sensible fluid flow	−7.6	−0.7
Hot-to-cold tank flow	Cold tank temperature	Sensible fluid flow	1.3	0.01
Process steam flow	Released power	TES feedwater flow	1.7×10^{-7}	2.1×10^{-8}
Peaking power	Peaking power	TES feedwater flow	1.1×10^{-7}	4.9×10^{-8}
Electrolyzer				
Electrolyzer temperature	Electrolyzer temperature	Electrolyte flow	−56	−0.42

lead to more aggressive responses to deviations between measured and setpoint values, while a larger K_i places greater emphasis on corrective action for accumulated errors.

References

[1] IEA. Energy technology perspectives 2020. International Energy Agency, Paris, France; 2020.
[2] Masson-Delmotte V, Zhai P, Pörtner H-O, Roberts D, Skea J, Shukla PR, et al. Global Warming of 1.5 °C: IPCC special report on impacts of global warming of 1.5 °C above pre-industrial levels in context of strengthening response to climate change, sustainable development, and efforts to eradicate poverty. 2022.
[3] IEA. Net zero by 2050. International Energy Agency, Paris, France; 2020.
[4] Mlilo N, Brown J, Ahfock T. Impact of intermittent renewable energy generation penetration on the power system networks – a review. Technol Econ Smart Grids Sustain Energy 2021;6(1):25. http://dx.doi.org/10.1007/s40866-021-00123-w.
[5] NEA. The costs of decarbonisation: system costs with high shares of nuclear and renewables. Nuclear Energy Agency, Paris, France; 2019.
[6] NEA. Technical and economic aspects of load following with nuclear power plants. Nuclear Energy Agency, Paris, France; 2011.
[7] NEA. Small modular reactors: challenges and opportunities. Nuclear Energy Agency, Paris, France; 2021.
[8] Ruth MF, Zinaman OR, Antkowiak M, Boardman RD, Cherry RS, Bazilian MD. Nuclear-renewable hybrid energy systems: Opportunities, interconnections, and needs. Energy Convers Manage 2014;78:684–94. http://dx.doi.org/10.1016/j.enconman.2013.11.030.
[9] Bragg-Sitton SM, Boardman R, Rabiti C, O'Brien J. Reimagining future energy systems: Overview of the US program to maximize energy utilization via integrated nuclear-renewable energy systems. Int J Energy Res 44(10):8156–69. http://dx.doi.org/10.1002/er.5207.
[10] IAEA. Guidance on nuclear energy cogeneration. no. NP-T-1.17. Nuclear energy series, 2019.
[11] DOE. Hybrid nuclear-renewable energy systems, quadrennial technology review 2015, chapter 4. Tech. rep., 2015.
[12] Frick K, Doster JM, Bragg-Sitton SM. Design and Operation of a Sensible Heat Peaking Unit for Small Modular Reactors. Nucl Technol 2019;205(3):415–41. http://dx.doi.org/10.1080/00295450.2018.1491181.
[13] Zhao B-C, Cheng M-S, Liu C, Dai Z-M. Conceptual design and preliminary performance analysis of a hybrid nuclear-solar power system with molten-salt packed-bed thermal energy storage for on-demand power supply. Energy Convers Manage 2018;166:174–86. http://dx.doi.org/10.1016/j.enconman.2018.04.015.
[14] Garcia HE, Mohanty A, Lin W-C, Cherry RS. Dynamic analysis of hybrid energy systems under flexible operation and variable renewable generation – Part I: Dynamic performance analysis. Energy 2013;52:1–16. http://dx.doi.org/10.1016/j.energy.2013.01.022.
[15] Dynamic analysis of hybrid energy systems under flexible operation and variable renewable generation – Part II: Dynamic cost analysis. Energy 2013;52:17–26. http://dx.doi.org/10.1016/j.energy.2012.11.032.
[16] Kim JS, Boardman RD, Bragg-Sitton SM. Dynamic performance analysis of a high-temperature steam electrolysis plant integrated within nuclear-renewable hybrid energy systems. Appl Energy 2018;228:2090–110. http://dx.doi.org/10.1016/j.apenergy.2018.07.060.
[17] Hills S, Dana S, Wang H. Dynamic modeling and simulation of nuclear hybrid energy systems using freeze desalination and reverse osmosis for clean water production. Energy Convers Manage 2021;247:114724. http://dx.doi.org/10.1016/j.enconman.2021.114724.
[18] Epiney AS, Rabiti C, Talbot PW, Kim JS, Bragg-Sitton SM, Richards J. Case Study: Nuclear-Renewable-Water Integration in Arizona. 2018, http://dx.doi.org/10.2172/1495196.
[19] Arent DJ, Bragg-Sitton SM, Miller DC, Tarka TJ, Engel-Cox JA, Boardman RD, et al. Multi-input, multi-output hybrid energy systems. Joule 2021;5(1):47–58. http://dx.doi.org/10.1016/j.joule.2020.11.004.
[20] GIF NEANH Task Force members. Position Paper on Non-Electric Applications of Nuclear-Heat: A Generation IV International Forum Priority. 2022.
[21] TANDEM Project official website, https://tandemproject.eu.
[22] Mattsson SE, Elmqvist H. Modelica - An International Effort to Design the Next Generation Modeling Language. IFAC Proc Vol 1997;30(4):151–5. http://dx.doi.org/10.1016/S1474-6670(17)43628-7, 7th IFAC Symposium on Computer Aided Control Systems Design (CACSD '97), Gent, Belgium, 28-30 April.
[23] IAEA. Nuclear–renewable hybrid energy systems. no. NR-T-1.24. Nuclear energy series, 2023.
[24] Cammi A, Casella F, Ricotti ME, Schiavo F. Object-Oriented Modeling, Simulation and Control of the IRIS Nuclear Power Plant with Modelica. 2005, p. 423–32.
[25] Casella F, Leva A. Modelling of thermo-hydraulic power generation processes using Modelica. Math Comput Model Dyn Syst 2006;12(1):19–33. http://dx.doi.org/10.1080/13873950500071082.
[26] ELSMOR Project official website, http://www.elsmor.eu.
[27] Chénais J, Douveneau A. Les SMR - Enjeux et avancées - Le projet SMR NUWARD™. 2020.
[28] IAEA. Status report – NUWARD (EDF lead consortium). Tech. rep., 2019.
[29] Haratyk G, Shirvan K, Kazimi M. Compact steam generator for nuclear application. In: Proceedings of NURETH16. 2015.
[30] Coleman JL, Bragg-Sitton SM, Dufek EJ. An Evaluation of Energy Storage Options for Nuclear Power. 2017, http://dx.doi.org/10.2172/1372488.
[31] Kuravi S, Trahan J, Goswami DY, Rahman MM, Stefanakos EK. Thermal energy storage technologies and systems for concentrating solar power plants. Prog Energy Combust Sci 2013;39(4):285–319. http://dx.doi.org/10.1016/j.pecs.2013.02.001.
[32] Mikkelson D, Frick K, Bragg-Sitton S, Doster J. Phenomenon Identification and Ranking Table Development for Future Application Figure-of-Merit Studies on Thermal Energy Storage Integrations with Light Water Reactors. Nucl Technol 2022;208(3):437–54. http://dx.doi.org/10.1080/00295450.2021.1906473.
[33] Bauer T, Odenthal C, Bonk A. Molten salt storage for power generation. Chem Ing Tech 2021;93(4):534–46. http://dx.doi.org/10.1002/cite.202000137.
[34] NEA. The role of nuclear power in the hydrogen economy: cost and competitiveness. Nuclear Energy Agency, Paris, France; 2022.
[35] Abdin Z, Webb C, Gray EM. Modelling and simulation of an alkaline electrolyser cell. Energy 2017;138:316–31. http://dx.doi.org/10.1016/j.energy.2017.07.053.
[36] Ulleberg Ø. Modeling of advanced alkaline electrolyzers: A system simulation approach. Int J Hydrogen Energy 2003;28(1):21–33. http://dx.doi.org/10.1016/S0360-3199(02)00033-2.
[37] Lange H, Klose A, Lippmann W, Urbas L. Technical evaluation of the flexibility of water electrolysis systems to increase energy flexibility: A review. Int J Hydrogen Energy 2023;48(42):15771–83. http://dx.doi.org/10.1016/j.ijhydene.2023.01.044.
[38] Cammi A, Ricotti ME, Casella F, Schiavo F. New Modelling Strategy for IRIS Dynamic Response Simulation. In: Proceedings 5th international conference on nuclear option in countries with small and medium electricity grids. 2004, p. 1–15.
[39] Pini A. A control oriented model for pressurizer transient dynamics. Politecnico di Milano; 2013.
[40] Barroso A, Baptista B, Arone I, Macedo L, Sampaio P, Moraes M. IRIS Pressurizer Design. 2003.
[41] Dittus F, Boelter L. Heat transfer in automobile radiators of the tubular type. Int Commun Heat Mass Transfer 1985;12(1):3–22. http://dx.doi.org/10.1016/0735-1933(85)90003-X.
[42] Kandlikar S. A General Correlation for Saturated Two-Phase Flow Boiling Heat Transfer Inside Horizontal and Vertical Tubes. J Heat Transfer 1990;112:219–28. http://dx.doi.org/10.1115/1.2910348.

[43] Mynatt FR, Townsend L, Williamson M, et al. Design and layout concepts for compact, factory-produced, transportable, Generation IV reactor systems. 2003, http://dx.doi.org/10.2172/817548.
[44] Bowman C, Bowman S. Thermal engineering of nuclear power stations: Balance-of-plant systems. 2020, http://dx.doi.org/10.1201/9781003011606.
[45] Ponciroli R, Bigoni A, Cammi A, Lorenzi S, Luzzi L. Object-oriented modelling and simulation for the ALFRED dynamics. Prog Nucl Energy 2014;71:15–29. http://dx.doi.org/10.1016/j.pnucene.2013.10.013.
[46] IAEA. Non-baseload operation in nuclear power plants: load following and frequency control modes of flexible operation. no. NP-T-3.23. Nuclear energy series, 2018.
[47] Heo JY, Park JH, Chae YJ, Oh SH, Lee SY, Lee JY, et al. Evaluation of various large-scale energy storage technologies for flexible operation of existing pressurized water reactors. Nucl Eng Technol 2021;53(8):2427–44. http://dx.doi.org/10.1016/j.net.2021.02.023.
[48] Frick K, Alfonsi A, Rabiti C, Bragg-Sitton S. Development of the IES plug and-play framework. INL/EXT-21-62050. Rev 00, Idaho National Laboratory; 2021, http://dx.doi.org/10.2172/1830013.
[49] Hammoudi M, Henao C, Agbossou K, Dubé Y, Doumbia M. New multi-physics approach for modelling and design of alkaline electrolyzers. Int J Hydrogen Energy 2012;37(19):13895–913. http://dx.doi.org/10.1016/j.ijhydene.2012.07.015.
[50] Gambou F, Guilbert D, Zasadzinski M, Rafaralahy H. A comprehensive survey of alkaline electrolyzer modeling: Electrical domain and specific electrolyte conductivity. Energies 2022;15(9).
[51] Chebac R. Preliminary power plant simulator for modelling of hybrid systems scenarios. Politecnico di Milano; 2020.
[52] Åström K, Hägglund T. PID controllers: theory, design, and tuning. ISA - The Instrumentation, Systems and Automation Society; 1995.
[53] Tripodo C, Lorenzi S, Cammi A. Definition of model-based control strategies for the molten salt fast reactor nuclear power plant. Nucl Eng Des 2021;373:111015. http://dx.doi.org/10.1016/j.nucengdes.2020.111015.